

Nanomedicine-Based Targeted Drug Delivery for Cancer Treatment

Bapu R. Thorat ^{1,*} , Devidas S. Bhagat ^{2,*} , Vilas A. Chavan ^{2,3,4} , Swati Wavhal ⁵ 

¹ Department of Chemistry, Government Arts and Science College, MS, Chhatrapati Sambhajnagar, 431001, India

² Department of Forensic Chemistry and Toxicology, Government Institute of Forensic Science, Chhatrapati Sambhajnagar-431 004, MS, India

³ Aditya University, Aditya Nagar, ADB Road, Surampalam, Kakinada District, 533 437, Andhra Pradesh, India

⁴ Department of Forensic Science, Parul Institute of Applied Sciences, Parul University, Vadodara, 391 760, Gujarat, India

⁵ Government of Maharashtra's Ismail Yusuf College of Arts, Commerce and Science, Mumbai 400 060, (MS), India

* Correspondence: devidas.bhagat@mah.gov.in;

Received: 24.06.2023; Accepted: 7.01.2024; Published: 25.11.2025

Abstract: Irrespective of the complex underlying principles of carcinogenesis and tumor metastases, as well as the drawbacks commonly associated with already-used cancer treatment options, successful cancer therapy remains a key concern for current medical research. Nanotechnology has been employed in cancer therapy and has huge potential for cancer treatment. Using knowledge of current breakthroughs in cancer hallmarks, we could comprehensively assess the pharmacological effects and examine the interactions between nanomaterials, thereby presenting prospects for developing nanomedicine-based mechanisms to treat malignancies in humans through targeted drug delivery. Nanomedicine's effective debut has demonstrated significant potential to improve cancer treatment strategies. Nanoparticles' unique properties, such as their ideal size, shape, effective surface-to-volume ratio, and surfaces that can be optimally customized, make them highly appealing delivery candidates for extremely hydrophobic drugs used in chemotherapy. Furthermore, their natural ability to encapsulate these medications and improve their solubility profiles provides them with unique benefits over traditional therapies. Surface enhancement with targeted ligands, enhanced intracellular uptake, and a longer in vivo circulation profile demonstrate their overall efficacy compared with alternative treatment methods. This article provides a biologist with an overview of nanotechnology and examines the benefits of several nanomedicines for targeted drug delivery in cancer treatment. The information presented in this review may be valuable for future research on developing effective nanomedicines for cancer treatment.

Keywords: nanomedicine; targeted drug delivery; nanomaterial; chemotherapy; cancer treatment.

© 2025 by the authors. This article is an open-access article distributed under the terms and conditions of the Creative Commons Attribution (CC BY) license (<https://creativecommons.org/licenses/by/4.0/>), which permits unrestricted use, distribution, and reproduction in any medium, provided the original work is properly cited. The authors retain copyright of their work, and no permission is required from the authors or the publisher to reuse or distribute this article, as long as proper attribution is given to the original source.

1. Introduction

There are some problems with the development and progress of effective diagnostics and treatments in medicinal chemistry, such as nonspecific drug accumulation, poor drug bioavailability, drug degradation during absorption and distribution, cytotoxicity, and the lack of early disease detection [1]. Some issues in effective cancer treatment include developing a multi-functional platform with specialized cancer cell targeting, high drug loading capacity, and adaptive drug release at the site of infection [2]. Polymer-based nanomaterials attract

significant attention across a broad range of applications, including the development of drug delivery systems [3]. A variety of biopolymers have been reported for the development of polymer-based nanocomposites with metal oxide nanoparticles. e.g. poly(lactic acid) (PLA), chitosan, poly(ϵ -caprolactone) (PCL), poly(hydroxyvalerate) (PHV), Poly(hydroxybutyrate) (PHB) and poly (*D,L*-lactic-co-glycolic acids) (PLGA) [4]. Glucose oxidase (GOx) was immobilized in Alg-MS in addition to tris(4,7-diphenyl-1,10-phenanthroline ruthenium (II) dichloride) (Rudpp) as an oxygen-sensitive dye utilized for glucose sensing, diclofenac sodium (Diclo) for anti-inflammatory activity, and citrate-coated magnetic nanoparticles made of Fe₃O₄ as an MRI agent [1]. A disk-shaped MCM-41 mesoporous material (pore size of 1.8 to 2.5 nm) was found to be a new, convenient reservoir for controlled drug delivery systems of ibuprofen, an extensively employed analgesic and anti-inflammatory drug [5]. The total drug loading capacity of MCM-41 is 30% by weight, and the drug-releasing behavior is dependent on the method of loading the drug, not on the use of surfactant for preparation. The maximum amount of the drug can be released into the solution/fluid after 3 days. There are two types of magnetic drug carrier nanomaterial/nanocomposites: (a) magnetic nanoparticles/composites incorporated with the active drug on the surface of the structure, (b) porous hollow magnetic capsules filled with active drugs and then sealed with lipids or other polymeric material to avoid the leakage of the drug in the bloodstream [6]. In terms of drug-loading capacity and drug-release efficacy, the latter approach was found to be preferable to the former. Because most active medications are hydrophobic, they can be simply encapsulated in a capsule, but nanoparticles require surface modification to absorb water-soluble drugs.

A poly(ϵ -caprolactone) (PCL) microspheres-magnetic nanoparticles made of Fe₃O₄ and anti-cancer medication doxorubicin hydrochloride (DOX) were synthesized and characterized using a modified solvent-evaporation approach [7]. Magnetic resonance imaging and a regulated medication delivery mechanism are two essential properties of these magnetic microsphere composites. Different aspects of drug-loaded nanocomposite microspheres were examined, including drug loading capacity, drug release at different pH levels, and in vitro cytotoxicity against HeLa cell lines. Microcomposites had drug-loading and encapsulation efficiencies of 36.7% and 25.8%, respectively. The pH-dependent drug-releasing capability and magnetic response of the drug-loaded microspheres are intriguing. DOX releases slowly at neutral conditions (pH 7.4), around 62% of the total loaded medication in 30 days, but DOX releases almost 86% in the comparable period at acidic conditions (pH 4.0). MTT assay against HeLa cells suggests that the drug-loaded microspheres are a potential DDS for drug storage and that delivering them to a specific site causes cell death in cancer cells. Further, a graphene oxide hybrid (GO-G3) microsphere compound was created by placing a core (G3, third-generation dendrimer made from citric acid as well as 1,3,5-benzene tricarbonyl trichloride) over a modified graphene oxide surface and testing its cytotoxicity against T47D cells [8]. In an acidic medium (pH 4), the graphene oxide hybrid (GO-G3) emitted green fluorescence at 471 nm, making it a viable drug carrier for cancer treatment. The graphene oxide hybrid (GO-G3) drug encapsulation capability for the anti-cancer medication doxorubicin (DOX) was 159.48%, while the drug release mechanism of this composite was pH dependent, releasing the drug more selectively in an acidic medium. Graphene oxide hybrid (GO-G3)-DOX composite cytotoxicity against T-47D cells (human breast cancer cells) has been shown by IC₅₀ values of 12.02 μ g/ml. Figure 1 shows the chemical structure of the alginate matrix, including monomers and polymer chains.

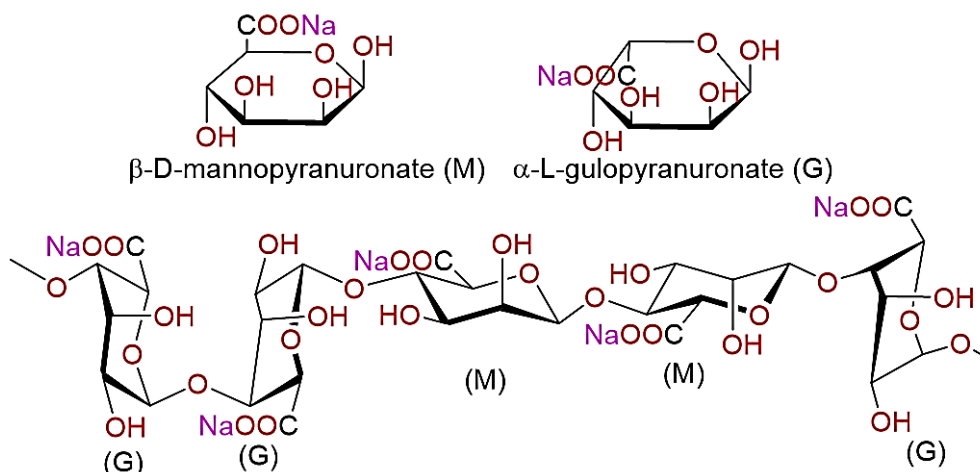


Figure 1. Chemical structure of the alginate matrix: monomers and polymer chain.

The graphene-poly(vinylpyrrolidone) nanoparticle combination was synthesized by the exfoliation of sheets of graphene utilizing poly(vinylpyrrolidone) nanoparticles of a mean size of 42 nm and assessed their anti-cancer efficacy (against HeLa, SCC-9, HCT-116, NIH-3T3, along with HEK-293 cell lines) and pH-sensitive drug delivery role for the anti-cancer drug doxorubicin [9]. The supramolecular collision was used to load DOX into the nanosheets. DOX's maximal release was observed at low pH and in an atmosphere with low oxygen content. These composites have dual functionalities and are being investigated for the cytotoxic process that drives cancer cell killing.

By combining Fe_3O_4 nanorods with $\text{Cu}_3(\text{BTC})_2$ nanocrystals, a novel magnetic porous metal-organic-framework (MOF)-based nanocomposites called $\text{Fe}_3\text{O}_4/\text{Cu}_3(\text{BTC})_2$ nanocomposite were created. Nimesulide, an anti-cancer drug that works as a specific cyclooxygenase-2 (COX-2) inhibitor, was then added [10]. Targeted drug administration, magnetic separation, and magnetic resonance imaging were all accomplished using these nanocomposites. The entire drug release in physiological saline at 37°C required about 11 days for this composite to absorb 0.2 g of nimesulide (NIM), a chemotherapy drug used to treat pancreatic cancer.

For the development of new drug delivery systems (DDS) for anti-cancer drugs and the creation of efficient cancer therapies, certain receptors on the surface of cancer cells, as well as unusual behavior and physicochemical conditions in the cancer/tumor environment (acidic pH, redox conditions, and elevated temperature), are key considerations. The DDS loaded with an anti-cancer medication is an efficient treatment that addresses several issues with anti-cancer medications, including nonspecific distribution, high levels of toxicity, poor solubility, and unstable solubility. For cancer therapy, a variety of DDSs can be used, including synthetic polymers such as poly(vinyl alcohol), poly(ethylene glycol), and poly(2-hydroxyethyl methacrylate), as well as natural polymers such as fibrin, collagen, alginate, agarose, and hyaluronan [11]. Natural polymers can be used as carriers because they offer many physicochemical benefits, including good biocompatibility, facile cellular uptake, biodegradability, greater hydrophilicity, and easy modification via basic chemical processes. They are also highly tunable within their cores, making them ideal for chemically conjugating or physically encapsulating drugs [12]. Despite its minimal toxicity, excellent biocompatibility, significant loading capacity, adaptability to environmental variables, and active functional groups for chemical changes, one of the natural polymers, chitosan (natural polysaccharide polymer), and its analogs, have attracted the most consideration as DDS for targeted

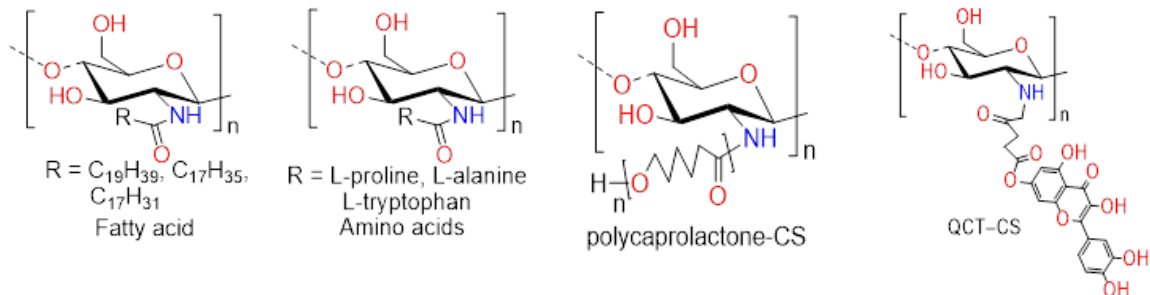
administration of various anti-cancer drugs to the tumor cells [13]. To enhance the CS polymer skeleton's characteristics related to the anti-cancer drug delivery process, several organic modifications were made to the CS skeleton using covalent bonds, including hydrophobic and hydrophilic groups, stimuli-responsive (pH, redox, and thermo) intended systems, and targeted ligands (peptides, protein/antibodies, tiny molecules, aptamers, and hyaluronic acid (HA)) [14]. These CS derivatives have been encapsulated or adsorbed via their nucleophilic free amine or hydroxyl groups, making them suitable for a variety of ligands, including pH-responsive bonds/groups/polymers, hydrophilic groups, hydrophobic groups, redox-responsive bonds, and other cell-targeting ligands. The hydrophobicity and biocompatibility of the CSs are improved by N-acylation and alkylation [15]. CS was subjected to an N-acylation utilizing acetic, butyric, or heptanoic anhydride. To ensure the compound's therapeutic efficacy, several acylated derivatives were prepared by selecting the acylating group while considering the degree of substitution and drug loading efficiency [16]. When combined with CS, 3,6-O, O'-dimyristoyl chitosan (DMCS) composite improves paclitaxel's (PTX) water solubility and cell permeability. This combination was risk-free, very minimally toxic to Caco-2 cells, and had excellent drug accessibility [17]. Some other hydrophobic materials including fatty acids like stearic acid (SA) [18], linoleic acid [19], palmitic acid [20], Caproic acid [21] and arachidic acid [22]; some hydrophobic amino acids like L-alanine, L-proline and L-tryptophan [23], arginine [24], N-acetyl-L-cysteine [25]; polycaprolactone micelles (for the delivery of PTX [26], 5-fluorouracil [27], siRNA and Curcumin [28]; quercetin (QCT) [29]; CS-pentyl trimethylammonium bromide [30]; N, N-diethyl ethylamine [31]; mPEG [32]; N-(2-hydroxy)-propyl-3- trimethylammonium chloride [33] were grafted over native CS by EDC and NHS method for the selective drug delivery. Table 1 presents modified CS/chitosan oligosaccharide (CSO) derivatives for drug delivery, including anti-cancer drugs. Figure 2 illustrates the structures of modified CS/chitosan oligosaccharides (CSO) derivatives used for delivering drugs.

Table 1. Modified CS/chitosan oligosaccharides (CSO) derivatives for the delivery of drugs and anti-cancer drugs.

Sr. No	Chitosan oligosaccharide derivatives	Active ligand	Active agent	Cell line	Results	Reference
1	3, 6-O, O'- dimyristoyl - chitosan (DMCS)	3, 6-O, O'- dimyristoyl	PTX	caco-2 cells	Improved PTX permeability with DMCS micelles, improved water solubility, and less toxicity to Caco-2 cells, and it is used to give PTX orally.	[17]
2	NH-fatty acids-CS: (DOX-CSO-SA)	Stearic (SA) acid	DOX	Breast cancer cells, multidrug resistant (MCF-7/Adr) cells	In comparison to commercial doxorubicin-HCl injection, DOX-CSO-SA micelles showed pH-dependent DOX release behavior, efficiently and evenly suppressed tumor growth, and reduced animal body toxicity.	[18]
3	Linoleic acid (LA)- grafted chitosan oligosaccharide (DOX-loaded CSO-LA micelles)	Linoleic acid	Doxorubicin (DOX)	--	The in vitro dispersion of the drug from the DOX-loaded CSO-LA micelles decreased by increasing the graft ratio of CSO-LA, which was used as a medium for hydrophobic medicines to improve their delivery. Drug encapsulation efficiencies (EE) of DOX-loaded CSO-LA particles were as high as nearly 75%.	[19]
4	Fatty acid-g-CS/DNA polyplex	Palmitic acid	Genetic material	--	Amphiphilic fatty acid-g-CS polymers can be employed as possible nonviral delivery	[20]

Sr. No	Chitosan oligosaccharide derivatives	Active ligand	Active agent	Cell line	Results	Reference
					systems for gene vectors in gene therapy because they form nano-CM with a small positive charge, demonstrate great hemo- and cytocompatibility, and have surfaces modified with ligands for selective targeting, improved cell binding, and internalization.	
5	Caproic acid grafted chitosan (CGC)	Caproic acid	Genetic material	--	The diversity of caproic acid substitution affects the effectiveness of gene transfection. A promising nonviral delivery system for gene vectors is the CGC-15 graft polymer.	[21]
6	DOX-Chitosan oligosaccharide–arachidic acid (CSOAA)	Arachidic acid	DOX	FaDu cells, FaDu tumor	When utilized to create self-assembled nanomaterials for anti-cancer drug delivery, DOX-loaded CSOAA-based nanomaterials demonstrated a pH-dependent drug release, little cytotoxicity in FaDu, human head, and neck cancer cells, and improved cellular absorption of DOX.	[22]
7	NH-amino acids-CS	L-alanine, L-proline, L-tryptophan	letrozole (LTZ)	--	ACNs encircled by LTZ exhibit various loading capacities, regulated drug release patterns, and encapsulation effectiveness, making them ideal drug delivery vectors.	[23]
8	N-Arginine CS (Arg-CS)	N-acetyl histidine	DOX	Breast tumor cell (MCF-7)	Due to improved cellular uptake, DOX-encapsulated NPs demonstrated pH-sensitive behavior and effectively killed the tumor cell line in a dose- and time-dependent manner.	[24]
9	Arg-CS	Octyl (oct)	Gambogic acid (GA)	Liver cancer cell (HepG2)	Oct-Arg-CS is a matrix for GA administration to increase anti-cancer action and extend half-life. Hepatic cancer is treated with oct-Arg-CS.	[24]
10	N-acetyl-L-cysteine CS	DA	QCT	A549	In addition to improving QCT's solubility in water and biocompatibility, QCT-loaded self-assembled amphiphilic CS nanomicelles additionally demonstrated greater inhibition rates than unloaded QCT.	[25]
11	Chitosan-grafted-polycaprolactone (CS-g-PCL) [PTX-loaded CS-g-PCL micelles]	Polycaprolactone	PTX	CaCo-2 and HT29-MTX intestinal epithelial cells	PTX permeability was greater in the CaCo-2/HT29-MTX co-culture model compared to the CaCo-2 monolayer, acting as a platform for dispensing PTX at the sites of absorption as well as a possible drug carrier for the intestinal administration of hydrophobic medicines (anti-cancer therapies). Association efficiency is as high as 82%.	[26]
12	5-fluorouracil loaded-CS-g-PCL	Polycaprolactone	5-fluorouracil	A549 cells	Self-assembled into micelles as DDS, the drug gets released in a controlled manner, and discharge half-time could reach up to 54.46 h, which is considerably shorter than that of free 5-Fu. Additionally, the drug has good biocompatibility as measured by cellular apoptosis and cytotoxicity evaluation.	[27]
13	Chitosan–BSA–TPP nanoparticles	Polyanion triphosphate (TPP)	BSA	--	Protein is released and transferred by bursts that are produced as a result of surface protein desorption and migration from sublayers, independent of particle size and shape.	[28]
14	QCT–CS	Quercetin	DOX	Caco-2 monolayer cells	The cellular internalization and penetration of DOX in Caco-2 monolayer cells are improved by the high drug encapsulation	[29]

Sr. No	Chitosan oligosaccharide derivatives	Active ligand	Active agent	Cell line	Results	Reference
					efficiency (about 89%) and prolonged release pattern in GSF (pH 1.2/pH 7.4).	
15	CS-pentyl trimethyl-ammonium bromide	Dodecyl aldehyde (DOA)	QCT	MCF-7	Biocompatible NPs carrying QCT displayed pH-sensitive behavior, accumulated on cell surfaces, and inhibited MCF-7 similarly to free QCT.	[30]
16	N, N-diethyl ethylamine CS	DOA	QCT	MCF-7	The QCT-loaded NPs' pH-responsive system demonstrated a synergistic effect on the regulation of breast cancer cells' survivability.	[31]
17	CS-mPEG	DA	Damnac-anthal (Dam)	Human osteosarcoma cell (U2OS)	Dam's in vitro release analysis is pH-dependent, and drug-loaded micelles had similar cytotoxicity to Dam's solution.	[32]
18	CS-Mpeg	Oleic acid	Camptothecin (Cam)	--	Typical size of 140 nm, a positive surface charge, excellent drug-loading efficiency, low Cam release in gastric medium, regulated release in intestinal fluids, and drug protection from hydrolysis in simulated gastrointestinal fluids (SGF) are all characteristics of polymeric micelles.	[32]
19	N-(2-hydroxy)-propyl-3-trimethyl-ammonium chloride/CS	Myristoyl chloride	CUR	Caco-2 and HT29-MTX intestinal epithelial cells	CUR-loaded and unloaded micelles had less cytotoxicity than free CUR.	[33]
20	TPGS-g-CS	Trastuzumab	DTX	Breast cancer cell (SK-BR-3)	Human epidermal growth factor receptor type-2 (HER-2) was the target, and the drug showed cytotoxicity with improved cellular uptake, bioavailability, and extended half-life.	[34]
21	O-succinyl chitosan grafted pluronic® F127 (OCP)	anti-HER2	DOX	MCF-7	HER-2 receptor was the target, increasing cell uptake effectiveness with 74% encapsulation efficiency.	[35]
22	Citrus pectin-CS NPs (MCPCNPs)	Cetuximab (Cet)	CUR	Caco-2	Epidermal growth factor receptor (EGFR) was the target, and the result was increased cell uptake and an anti-cancer impact.	[36]
23	CMC-phenylboronic acid pinacol ester CMC-BAPE	CD147	DOX	HepG-2	Targeted CD147 sensors demonstrate better anti-cancer activity than controls, as well as high and quick drug release with good blood circulation stability.	[37]



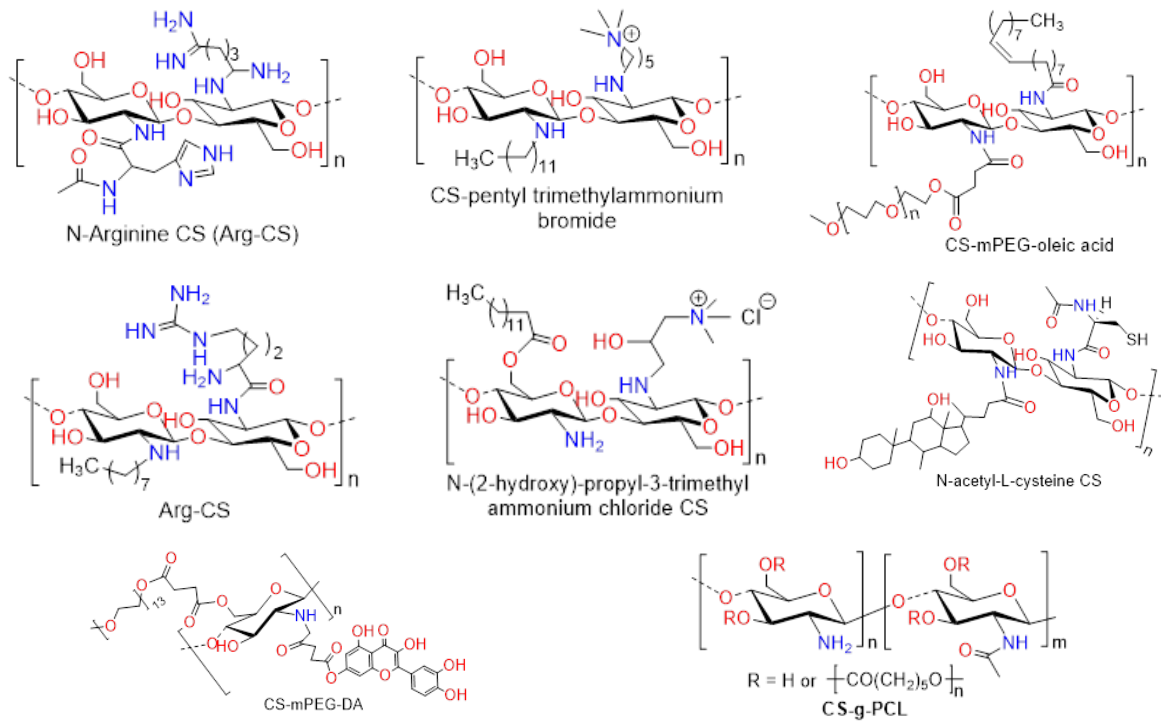


Figure 2. Structures of modified CS/chitosan oligosaccharides (CSO) derivatives for delivery of drugs.

Imatinib, an anti-cancer medicine, was loaded onto a biodegradable and biocompatible polyurethane (PU) that was created from several amino acids (as chain extenders). The loading efficiency was 94%. [38]. The hydrolytic degradation (20-38%) and swelling ability (4-13%) of all PUs were more significant. The pH of a loaded medicine affected how well it released the substance. Compared to acidic and basic pH, it releases a lower amount of medication at the physiological pH (7.4). Approximately 82% of the medication has been released at an acidic pH as opposed to 41% at pH 7.4. Cell viability was over 90% according to the MTT assay, which is within acceptable limits. Figure 3 displays the chemical structure of various polyurethanes (PUs).

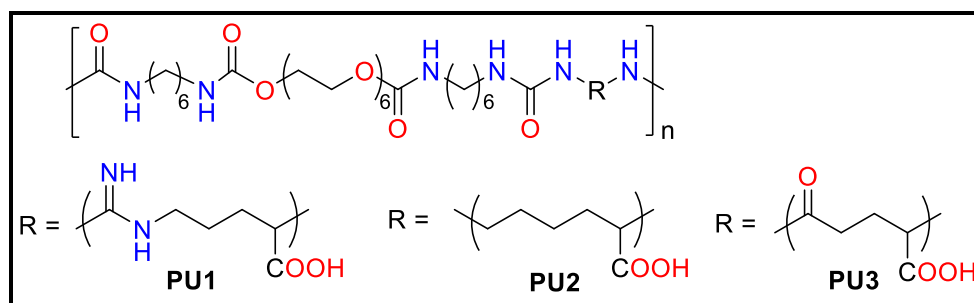


Figure 3. Chemical structure of different PUs.

Pure mesoporous silica nanoparticles were among the most intriguing delivery systems for targeting drugs, but their use is limited by their tendency to aggregate in physiological environments or in the presence of salt, and to bind nonspecifically to serum- or protein-containing solutions. The weakly water-soluble anti-cancer medication (hydrophobic) has improved water solubility and bioavailability in nanocomposites such as micelles@MSNs drug delivery systems [39]. DTAB (dodecyltrimethylammonium bromide), SDBS (sodium dodecylbenzene sulfonate), P123, F127, Nonidet P-40, and CTAB (cetyltrimethylammonium bromide) are highly effective anti-cancer agents and chemosensitizers used in MDR cancer therapies [40]. Doxorubicin, a weakly water-soluble anti-cancer drug, and a surfactant

chemosensitizer were readily combined with mesoporous silica nanoparticles (MSNs) via a one-pot co-self-assembly protocol involving the drugs, surfactant micelles, and silicon sources [41].

The composite's drug-releasing behavior is pH-dependent; it releases the drug in cancer cells rather than in normal tissues, where the pH is typically 7.2 to 7.5, via ion-exchange interactions between H^+/H_3O^+ and the electrophilic drug@micelles. As a result, the medication builds up inside cancer cells, causing multidrug combination chemosensitization to overcome MDR in cancer. Through a synergistic cell cycle arrest/apoptosis-inducing action between weakly water-soluble DOX and CTAB, the nano-MDDS DOX@CTAB@MSNs exhibit the maximum cytotoxicity over both drug-sensitive MCF-7 cells and drug-resistant MCF-7/ADR cells. These composites demonstrate passive targeting capabilities by utilizing the aberrant tumors' enhanced permeability and retention (EPR) effect. For the ligand-assisted selective delivery system and imaging agents, an intriguing PEGylated phospholipid coating and 13-(chlorodimethylsilyl-methyl)heptacosane (CDSMH)-derivatized MSNs were developed and described [42]. Figure 4 shows the structure of 13-(chloro-dimethyl-silyl-methyl)heptacosane (CDSMH). To accomplish ligand-assisted targeted administration, the medicinal agent folate or the imaging agent fluorescein isothiocyanate can be bound to the surface of phospholipids. After delivery, phospholipid-capped MSNs sensitized with folate promote selective cellular uptake by HeLa cells. The mesoporous silica nanoshuttles on HeLa cells have no discernible harmful effects. This new generation of lipid-capped MSN nanoshuttles was discovered to be an innovative drug carrier with potential clinical applications.

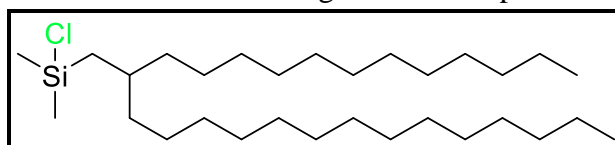


Figure 4. Structure of 13-(chloro-dimethyl-silyl-methyl)heptacosane (CDSMH).

A porous and luminescent β - $NaYF_4:Yb^{3+}, Er^{3+}$ @ SiO_2 nanocomposite was created by electrospinning luminous β - $NaYF_4:Yb^{3+}, Er^{3+}$ nanoparticles into unified mesoporous silica shells. The surface of the composites was then enhanced with cancer-targeting ligand folic acid (FA) and PEG. A typical UCNPs@m SiO_2 -PEG/FA nanosphere, measuring roughly 80 nm in size, has been disseminated in water. The produced multi-functional nanocomposite spheres can be used for cell imaging and anti-cancer medication delivery. Doxorubicin hydrochloride (DOX), an anti-cancer medication, can be added to the surface of UCNPs@m SiO_2 -PEG/FA nanospheres; the loading efficiency is 67%, and the drug loading percentage is 12%. In a PBS buffer solution at 37°C, DOX-loaded UCNPs@m SiO_2 -PEG/FA nanospheres have an *in vitro* drug release efficiency that is pH dependent. The medication releases more effectively at lower pH levels; after 4/48 hours, DOX releases 6% at pH 7.4, 21% at pH 5.5, and 34% at pH 2.0. The DOX-loaded UCNPs@m SiO_2 -PEG/FA nanospheres exhibit greater *in vitro* cell cytotoxicity when tested on cancer cells than free DOX and DOX-loaded UCNPs@m SiO_2 -PEG at the same concentrations, indicating that they may be used as anti-cancer carriers of drugs for anti-cancer activity. These composites are potential candidates for use as bioimaging agents since the upconversion luminescence image of UCNPs@m SiO_2 -PEG/FA taken up by cells exhibits green emission under 980 nm infrared laser excitation [43].

By employing $Y_2O_3:Yb^{3+}/Er^{3+}$ as templates, hollow-shaped cubic phase (α) $NaYF_4$ nanospheres with a mean particle size of < 200 nm were created, which offer more drug delivery possibilities [44]. Mesoporous α - $NaYF_4:(20\%)Yb^{3+}, (2\%)Er^{3+}$ nanoparticles

(HMNPs) with mesoporous shell and hollow interior structure were synthesized from $\text{Y}(\text{OH})\text{CO}_3:\text{Yb}^{3+}, \text{Er}^{3+}$ nanospheres via a surface-protected “etching” and hydrothermal ion-exchange process using polyethyleneimine (PEI) ligands, which played a major role in the creation of the hollow structured $\alpha\text{-NaYF}_4$ nanospheres. Folic acid, a substance used to treat cancer, is attached to a free amino group on the surface of nanoparticles (NPs). As carriers for anti-cancer medications, hollow NPs modified with FA were employed. When used against HeLa cells, DOX-loaded $\alpha\text{-NaYF}_4:\text{Yb}^{3+}, \text{Er}^{3+}$ NPs exhibit less cytotoxicity than DOX-loaded FA-modified $\alpha\text{-NaYF}_4:\text{Yb}^{3+}, \text{Er}^{3+}$ NPs. Under 980-nm infrared laser stimulation, this conjugate emits a brilliant green light with no background noise. These versatile hollow and mesoporous nanospheres have the potential to serve as cancer drug delivery systems and cell imaging agents [45].

An anti-cancer medicine called DOX was loaded into nanoscale Fe-Pt network hollow capsules (340 nm in size with large pores of 20 nm), which were subsequently coated with lipids and used as magnetic capsules for anti-cancer research. Without external stimulation, the aqueous anti-cancer medication was loaded into the hollow interior of the nanosized FePt capsules and released into cancer cells. Using an NdFeB magnet (0.2 T), the drug-loaded capsule-covered lipid membrane was effectively directed to cancer cells and killed over 70% of them (gastric cancer cell line MKN-74 and lung cancer cell line RERF-LC-A1) [46]. The target-oriented medication delivery system used FePt network capsules, which function as supermagnets at body temperature. There have also been reports of other nanomaterials, such as hollow microspheres with an Fe_3O_4 shell, used as magnetic capsules [47]. This shell's pore size was found to be too small for adequate drug filling and release, and it was too thick (>20 nm) to provide internal space for drug loading. As a result, the direct use of Fe_3O_4 shells as DDS is limited.

Cobalt ferrite (CoFe_2O_4) nanocrystals display excellent chemical and thermal stabilities; therefore, various kinds of nanocomposites such as $\text{CoFe}_2\text{O}_4@\text{TiO}_2$ [48], $\text{CoFe}_2\text{O}_4@\text{SiO}_2$ [49], $\text{CoFe}_2\text{O}_4@\text{C}$ [50], and $\text{CoFe}_2\text{O}_4@\text{MOF}$ [51] were reported for various applications. Due to their greater magnetic anisotropy than that of Fe_3O_4 nanoparticles, certain inorganic-plated (mesoporous silica-covered) cobalt nanoparticles derived from ferrite were relevant in medicine, particularly for magnetic-focused drug delivery systems [52]. Using a self-assembling technique, brand-new dual-functional magnetic nanoparticles made of CoFe_2O_4 with fibrous silica shells were produced. These nanocomposites have a mesoporous structure, spherical morphology, narrow size distribution, large surface area, excellent monodispersity, and superparamagnetic properties. The fibrous silica- CoFe_2O_4 nanocomposite is coated with the anti-cancer drug doxorubicin hydrochloride. These bifunctional nanocomposites have outstanding pH-sensitive drug release capabilities in addition to extremely high drug loading capacity. The DOX release rate from DOX- $\text{CoFe}_2\text{O}_4@\text{FMS}$ nanocomposites [53] increases with decreasing pH. At pH 7.4, only 22.4% DOX is released after 48 hrs., whereas it is 46.2% at pH 4.0 in the same duration of time. As a result, it can be used as a potential delivery mechanism for anti-cancer therapy in the HeLa cell line.

Silver nanoparticles (Ag NPs) have shown excellent antimicrobial activity in the past few years and are used in different medical products [54]. Green synthesis of silver nanoparticles (AgNPs, 36.66 ± 7.85 nm) was reported using *P. annua* extract, which contains desirable levels of flavonoids, phenols, and alkaloids that act as reducing and stabilizing agents

for AgNPs. These biogenic AgNPs were then coated with starch, operating as a composite drug delivery system for the anti-cancer medication [55].

To create an efficient targeting agent, small porous iron oxide nanorods (IOPNR) with pore sizes of 5 to 10 nm were coated with folic acid (FA) utilizing poly(ethylene glycol)-bis(amine) (NH₂-PEG-NH₂) as a spacer. These IOPNRs were generated by the hydrothermal technique and calcination [56]. The nanorods have been coated with poly(ethylene glycol), which improves the dispersibility of the nanoparticles and prolongs the circulation time of DDS by reducing plasma protein adsorption [57]. On the surface of FA-PEG-IOPNR, doxorubicin (DOX) was loaded into the pores. Drug release is accelerated in an acidic environment, for example, at pH 5.3, compared to neutral pH 7.4. In HeLa cells, a folate receptor (FR)-positive cell line, the coating of folic acid on the surface of nanorods improves the cellular uptake of nanorods. In contrast, it was found that the FA ligand on the nanorod surface did not affect cellular uptake in COS 7 cells, an FR-negative cell line. When tested on HeLa cells, the DOX-loaded FA-PEG-IOPNR exhibited greater cytotoxicity than the DOX-loaded PEG-IOPNR, whereas testing on COS 7 cells showed no discernible difference in cytotoxicity between the two composites. According to these findings, FA-PEG-IOPNR was discovered to be a powerful DDS for chemotherapeutic research into cancer cell lines [58].

Some iron oxide particles covered with LDHs replaced the traditional polymer-coated magnetic drug carrier. Numerous magnetic core-LDH shell nanocomposites have been shown to have anti-inflammatory properties [59]. Several spherical, submicron-sized doxifluridine-intercalated Fe₃O₄@LDH particles have been prepared [60], which are then incorporated with anti-cancer agents [61]. Most of the magnesium ferrite and magnetite nanomaterials have the core iron oxides-LDH shell composition [62]. The superparamagnetic calcium ferrite nanoparticles were coated with a biohybrid casein coating to increase surface area for drug encapsulation and for magnetically controlled release. To create casein-GNS-PG and casein-CFNP-GNS-PG, the NHS ester of PG combined two drug carriers: casein-GNS (GNS-genistein) and casein-CFNP-GNS. Using the MTT assay, the cytotoxic effect of these composites was assessed against the ovarian cancer cell line SKOV-3 and the TNBC cell line MDA-MB-231. Within 4 hours, this composite releases 93.21% of the medication while an external magnetic field is present. According to in vitro cytotoxicity data, genistein's anti-cancer potential was 140 times more effective, thanks to the progesterone-conjugated drug carrier system, which enabled selective and rapid cellular targeting [63]. Different compositions of ferromagnetic Fe₃O₄ nanomaterials were obtained via the treatment of nano-Fe₃O₄ with different surface modification reagents such as tetraethyl orthosilicate (TEOS), (3-aminopropyl)trimethoxysilane (APTMS), and alginate (AA), forming corresponding composites as Fe₃O₄@SiO₂, Fe₃O₄@SiO₂-NH₂, and Fe₃O₄@SiO₂-NH₂-AA nanoparticles, respectively [64]. These parameters are all met by the mesoporous silica-coated Fe₃O₄ nanoparticles, which also have strong biological potential. Silica serves as the protective outer layer of Fe₃O₄ particles, which have been identified as the most promising composites and meet the requirements for use as drug delivery system (DDS) carriers for specialized pharmaceuticals at specific sites in the human body [65]. Diagnostic and therapeutic agents can be readily encapsulated, covalently attached, or absorbed onto nanocomposites [66]. These composites show maximum adsorption of the alkaloids palmatine and berberine at pH 8. Nearly 22.2% of palmatine was absorbed, while 23.6% of berberine was absorbed at pH 8. However, the adsorption of both alkaloids was less in the liquid state at pH 7.

Some $\text{Fe}_3\text{O}_4@n\text{SiO}_2@m\text{SiO}_2$ composite nanoparticles with an average size of 400 nm were prepared, showing good adsorption and release properties (about 95 % in 85 hours) for ibuprofen [67]. A few hollow $\text{Fe}_3\text{O}_4@\text{SiO}_2$ sphere nanocomposites with an average size of 900 nm were created, and they demonstrated increased drug loading (aspirin loading) and sustained drug-releasing capacity [68]. However, it is unsuitable for targeted drug delivery because nanoparticles below 300 nm are preferentially used for this application [69]. Variable-thickness magnetite core and meso-silica shell nanocomposites were prepared via hydrothermal and sol-gel processes, and their ibuprofen adsorption, retention, and release, as well as cytotoxicity, were evaluated to assess biocompatibility with human tissue. $\text{Fe}_3\text{O}_4@m\text{-SiO}_2$ core-shell pores had an average size of ~ 2.16 nm. The biocompatibility of these composite materials for drug delivery applications is 80%. $\text{Fe}_3\text{O}_4@m\text{-SiO}_2$ nanocomposites exhibit good drug release behavior up to 81% of the loaded drug and can store as much as 954 mg per gram of sample [70]. Therefore, $\text{Fe}_3\text{O}_4@m\text{-SiO}_2$ nanocomposite can be used as a DDS (drug delivery system) for cancer and non-cancer therapy.

Ibuprofen was used as a model drug, and multi-functional $\text{Fe}_3\text{O}_4@m\text{SiO}_2\text{-AuNCs}$ composite nanoparticles were created as the DDS. This composite was created by coating luminous gold nanoclusters with mesoporous silica ($m\text{SiO}_2$) and magnetic Fe_3O_4 nanoparticles. The mesoporous silica layer was coated with AuNCs. Ibuprofen (IBU) was used to test the ability of $\text{Fe}_3\text{O}_4@m\text{SiO}_2\text{-AuNCs}$ composites to load and release drugs. The composites have a drug loading capacity of 32 mg/g at 40°C after 90 minutes at pH 7.4. At pH 7.4, the maximum amount of the medication (90%) was released, making this composite an excellent platform for multi-functional DDS [71].

Some special organic-inorganic hybrid thermo-sensitive composites as drug delivery systems were reported. Thermo-sensitive PNIPAAm/mesoporous silica nanocomposites were prepared by impregnation of NIPAAm monomers into the channels of SBA-15 and then underwent *in-situ* radical polymerization in mesopores. Ibuprofen, the model drug, was loaded onto the composite; the loading effectiveness of IBU depended on the amount of polymer in the composite. The loaded IBU content depended on the loading solution and temperature, i.e., on the interaction between polymers and IBU and on the trap effect of polymer chains. The release of IBU around the LCST was thermally controlled. By adjusting the corresponding dimensions of drug molecules and mesoporous routes, the amount of polymer in composites, the density of the polymer network, and the interactions between the drug and the polymer, it was possible to control both the efficiency and quantity of drug release. These novel drug carriers control drug release and have other applications [72]. Figure 5 depicts the interaction of loaded IBU with the PNIPAAm/SBA-15 composite.

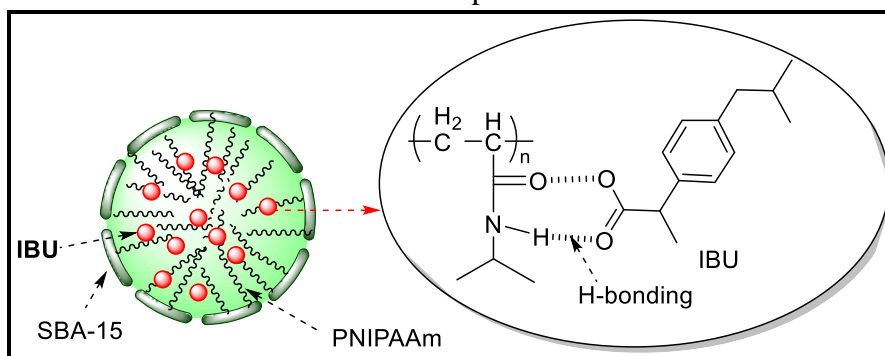


Figure 5. Interactions of loaded IBU with PNIPAAm/SBA-15 composite.

(P(NIPAAm-co-AAc)) Latex particles did not show an induced cytotoxicity effect and impact on the cell growth in the L929 cell in the presence of particles [73]. Nanoparticles below 200 nm have been reported as drug carriers for cancer therapy, stroke, and hypertension [74]. PNIPAAm-co-AAc latex particles were prepared via emulsion polymerization using SDS surfactant. The size of nanoparticles decreased with increasing surfactant concentration [75] and temperature. At 8 mM critical micelle concentration of SDS, nearly 59 nm latex nanoparticles were prepared. As temperature-sensitive drug carriers, these latex nanoparticles were employed to load 4-acetamido-phenol for study purposes. Smaller or AAc-rich hydrogel particles, among other factors, were exhibiting sustained drug release properties and may have significant biomedical applications [76].

As a brand-new anticancer drug carrier, novel spherical and nonspherical iron oxide@double hydroxide stacked core-shell nanocomposites were developed. The anti-cancer medicine "5-fluorouracil" (5FU) is combined with two different types of iron oxide@LDH core-shell structures: anisotropic Fe_2O_3 @Mg-Al-5FU-LDH and isotropic Fe_3O_4 @Mg-Al-5FU-LDH. Both have good drug-loading capacities (around 30%) and ferromagnetic properties. Regardless of their forms, each of these materials exhibits a variable in vitro drug release profile; an anisotropic carrier has been shown to have a higher release rate (about 80% around pH 7) [77]. Magnetically active mesoporous silica microparticles incorporating up to 11% by weight of γ - Fe_2O_3 nanoparticles were prepared, which showed excellent drug loading and release properties and were therefore used as vehicles for magnetic drug targeting [78]. Mesoporous silica nanoparticles were used as DDS because these particles have a large surface area and porosity, enabling them to accumulate, adsorb, or store large amounts of hydrophobic drugs. These particles have maximum cellular uptake. These materials have been used as cell markers [79], gene transfection reagents [80], drug-delivery vectors [81], and carriers of molecules [82]. Camptothecin (CPT) loaded onto fluorescent mesoporous silica nanoparticles (FMSNs) was found to be an effective composite for inducing apoptosis in cancer cells [83]. The drug molecule (CPT) remained within the nanocomposite and was effectively released into the cancer cell's hydrophobic region, exerting an apoptotic effect. The preferred route cannot be used to administer drugs that are insoluble or only sparingly soluble in water. In such cases, mesoporous silica nanoparticles are used as DDS for these drugs and control their release at infected sites, making them more effective than other DDS, such as PEGylated liposomal particles or albumin-based nanoparticles.

The anti-tumor model medication 5-fluorouracil (5-FU) was loaded onto a new magnetic Fe_3O_4 /graphene oxide (GO) nanocomposite [84]. The drug-loading capacity of the multifunctional Fe_3O_4 /GO nanocomposites was as high as 0.37 mg mg⁻¹ when the initial drug concentration was 0.5 mg mg⁻¹, and its drug-releasing behavior depended on the pH of the environment. Fe_3O_4 /GO/5-FU nanocomposites release only 21% of the drug under neutral conditions within 24 hours, whereas they release nearly 72% of the drug in acidic conditions. Due to a shift in hydrogen bonding interactions between Fe_3O_4 /GO and 5-FU, the drug releases more quickly under acidic conditions than under neutral conditions. As a result, it functions as a regulated drug-delivery system in the acidic microenvironments of malignant cells, minimizing drug leakage under physiologically appropriate conditions. As efficient covalent drug delivery systems for the transport of anti-cancer medication to MCF-7 breast cancer cells, new AuNPs-RGO nanocomposites have been developed. Through the use of an acid-cleavable amid bond (SMTX-AuNPs) and a 3-mercaptopropionic acid (MPA) spacer, the anti-cancer medication mitoxantrone (MTX) was grafted over gold nanoparticles. The surface of the RGO

nanosheets was then embellished with these composites. The pH has an impact on how effectively the composite releases drugs. SMTX-AuNPs, free MTX, and SMTX-AuNPs/RGO were tested for their ability to kill MCF-7 cells in vitro using the MTT assay, DAPI staining, DNA fragmentation assay, and gene expression analysis. Unlike free MTX and SMTX-AuNPs/RGO, SMTX-AuNPs demonstrated superior anti-cancer efficacy against the MCF-7 cell line [85]. The findings from this research are that RGO is not a good choice for covalent drug delivery systems. Figure 6 depicts the structure of SMTX.

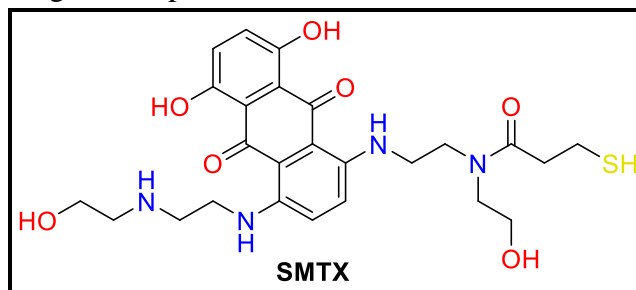


Figure 6. Structure of SMTX.

Folate receptor-targeted poly(amidoamine) (PAMAM) dendrimer-functionalized mesoporous silica-coated magnetic nanoparticles (Fe_3O_4) were developed as an innovative drug delivery system for photodynamic therapy (PDT). Their surface was coated with mesoporous silica (M-MSN), further customized with siloxane-cored PAMAM dendrons. Folic acid was used to target the M-MSN-PAMAM nanocarriers' surface before indocyanine green (ICG) dye was applied, and the drug-loaded nanocarriers were subsequently used in photodynamic treatment against MCF-7 cells. These cell cultures were exposed to 785 nm radiation for 20 minutes in the presence of an ICG-loaded M-MSN-PAMAM-FA composite. An in vitro study found that this compound induces apoptosis in the MCF-7 cell line [86]. Figure 7 depicts a two-dimensional view of the ICG-loaded M-MSN-PAMAM-FA composite.

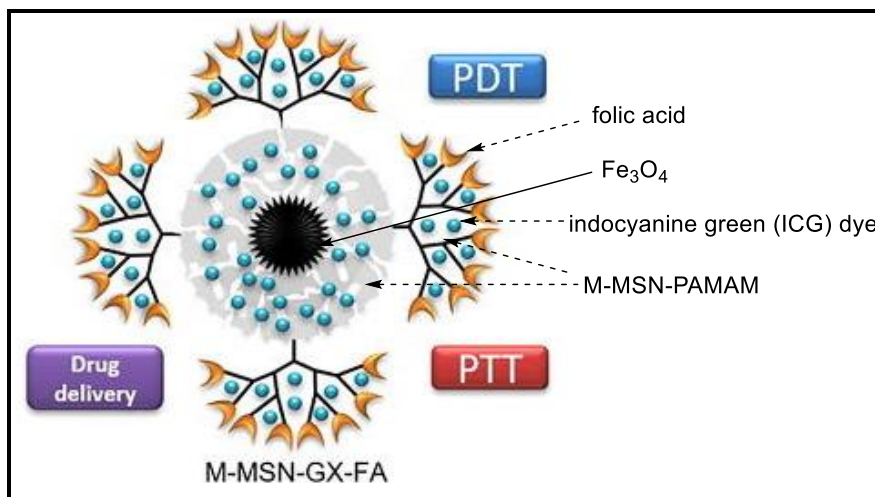


Figure 7. 2D view of the ICG-loaded M-MSN-PAMAM-FA composite.

Utilized as DDS for anti-TB medications are wheat germ agglutinin (WGA)-coated Lectin-functionalized poly (lactide-co-glycolide) nanoparticles (WGA-coated PLG-NPs) with an average size range of 350-400 nm [87]. Wheat germ agglutinin (WGA) is often bound to PLG-NPs in amounts of 3 to 3.5 μg per milligram. This composite's drug encapsulation efficiency ranges from 54-66%. To treat tuberculosis (TB), this composite was employed as a bioadhesive medication carrier. The drug loading efficiency of coated and uncoated PLG nanoparticles (isoniazid, rifampicin, and pyrazinamide) was essentially the same. Drugs are

more effective against tuberculosis because they remain in the body for 10 to 15 days after treatment, both in tissues and plasma. Three oral/nebulized doses of this formulation, given once every 15 days, were equivalent to 45 oral-free doses of three frontline anti-TB medications, reducing the quantity and frequency of these medications. Drug resistance is less likely to develop in organs when drug levels are higher than the minimum inhibitory concentration (MIC).

To effectively deliver medication to a specific site, novel poly(lactide-co-glycolide) nanoparticles (NPs) conjugated to anti-EGFR mAbs were developed [88]. In non-small-cell lung cancer (NSCLC), an antibody called EGFR was overexpressed and linked to poor differentiation, greater tumor growth, a poorer prognosis, and a greater likelihood of lymph node metastases [89]. Cet-DTX-NPs composites outperformed DTX-NPs composite and DTX in terms of antiproliferative effects on the A549 cells, according to an *in vitro* cytotoxicity analysis. Because Cet-DTX-NP composites improve intracellular drug levels and uptake efficiency, which (drug, Cetuximab) shows anti-EGFR activity, they exhibit increased activity. [90]. Around the nucleus, 6-coumarin PLGA NPs were gathered in the cytoplasm. Because Cetuximab binds to the EGFR receptor and delivers the drug to tumour cells, inducing significant synergism, the A549 cell line undergoes apoptosis, thereby inhibiting EGFR signalling. NPs containing mAb conjugations showed greater cytotoxicity and cellular absorption [91].

One intriguing biodegradable semicrystalline synthetic polymer, PVA, is employed directly or by modified methods in various biomedical applications. To increase the solubility of the required active substance, PVA is used directly to generate solid suspensions in most pharmaceutical formulations. Numerous *in vitro* and *in vivo* investigations show that PVA is a non-toxic, biocompatible polymer. A promising novel targeted therapy uses nanoparticles or microparticles encapsulated with drugs, hydrogels, etc., to deliver drugs to targeted sites. This is necessary due to several disadvantages and the restricted application of current therapy, including heterogeneous disease manifestations, higher doses, and their side effects. To create innovative DDS in the form of hydrogels, nanocomposites, nanoparticles, or microparticles for the therapeutic use of various infections, illnesses, and diseases, PVA was conjugated with its copolymers (biodegradable polymers) [92].

Combination chemotherapy, which delivers two or more anti-cancer medications simultaneously using nanomaterials, is presently the preferred method of drug administration in clinical practice. Intriguingly, the tumor's growth was decreased by the anti-cancer medications loaded on the nano-drug co-delivery system (NDCDS) compared to the free medications [93]. This is one practical method for loading two or more anti-cancer medications onto a delivery system. The medications should have distinct physicochemical and pharmacological mechanisms, as well as distinct toxicity and side effects [94]. A small-molecule medicine, a macromolecule anti-cancer agent, or two small-molecule anti-cancer therapies were used in some NDCDS cases [95]. Table 2 presents some nano-drug co-delivery systems containing small molecules that exhibit anti-cancer activity.

Table 2. Some nano drug co-delivery systems with small molecules show anti-cancer properties.

Sr. No.	Bio-nanomaterial	Type 1 drug	Type 2 drug	Indications	Reference
1	mPEG-PLGA	Doxorubicin	PTX	Non-small lung cancer, melanoma, hematoma	[96]
2	PCL-SS-CTS-GA micelle	Doxorubicin	CUM	Hematoma carcinoma	[97]
3	Polymer-lipid hybrid	Doxorubicin	Mitomycin C	Murine breast cancer	[98]

Sr. No.	Bio-nanomaterial	Type 1 drug	Type 2 drug	Indications	Reference
4	Pluronic F-127 diacrylate macromer	5-fluorouracil	Camptothecin		[99]
5	P(MDS-co-CES) micelle	Paclitaxel	Herceptin	Breast cancer	[100]
6	DSPE-PEG-AA/rHDL/DCA-PEI/p53	Dichloroacetate	p53	Lung adenocarcinoma	[101]
7	PLLA/PLGA	Doxorubicin	p53	Hepatocellular carcinoma	[102]
8	Polyamidoamine dendrimer functionalized graphene oxide	Doxorubicin	MMP-9 shRNA	Breast cancer	[103]
9	OEI600-PBA/HBPO	Doxorubicin	Beclin1 siRNA		[104]
10	FA/PEG/liposomes (EPC, CHOL, and DOTAP)	Paclitaxel	Tariquidar	Ovarian cancer	[105]
11	PLGA	Doxorubicin	Gambogic acid	Breast cancer	[106]
12	mPEG-g-PLL-b-Phe	Doxorubicin	P-gp siRNA	Breast adenocarcinoma	[107]
13	Nanoscale metal-organic frameworks	Cisplatin prodrug	MDR gene-silencing siRNAs (Bcl-2, P-gp, and survivin)	Ovarian cancer	[108]
14	Folate acid conjugated graphene oxide	Doxorubicin	Gold NPs		[109]
15	PLGA	Doxorubicin	Gold NPs		[110]
16	Metallo-supramolecular nanoge	Doxorubicin	Tetraphenylporphyrin zinc		[111]
17	Mesoporous silica	Doxorubicin	Gold nanorods	Lung carcinoma	[112]
18	Liposomes (EPC, CHOL, DOTAP, PEG2kPE)	Paclitaxel	Tariquidar	Ovarian cancer	[113]
19	Transferrin conjugated Liposomes	Doxorubicin	VER	Leukemia	[114]
20	FA-PEG-PLGA	cis-Diaminodichloroplatinum	PTX	Non-small lung cancer	[115]
21	β -CD modified CdSe/ZnSe QDs coupled to L-Arg or L-His	Doxorubicin	siRNA targeting the MDR1 gene	Cervical cancer	[116]
22	Gold nanorod	Doxorubicin	siRNA against ASCL1	Neuroendocrine carcinoma	[117]
23	poly(styrene-co-maleic anhydride) derivative with adipic dihydrazide	Doxorubicin	Disulfiram	Breast cancer	[118]

3. Discussion

Several studies have successfully developed highly effective nanocarriers for delivering nanomedicine into cancer cells. Tests conducted both in vitro and in vivo demonstrated that the therapeutic drug was successfully co-delivered to cancer cells. Additionally, delivering chemotherapeutic drugs to cancer cells using nanoparticles can achieve high drug concentrations within cancer cells while reducing side effects. Above all, drug resistance can be eliminated using nano-carrier-based methods for chemo-drug co-delivery. Recently, researchers have looked into several "smart" nanoparticles having the capacity to react to both internal and external stimuli.

There is significant interest in polymer-based nanoparticles for a variety of applications, including the development of drug delivery systems. A wide variety of biopolymers have been characterized for the creation of polymer-based nanocomposites containing metal oxide nanoparticles. In addition, a disk-shaped MCM-41 mesoporous material was demonstrated to

be a new effective reservoir for ibuprofen, a widely used analgesic and anti-inflammatory drug, and controlled drug delivery systems. In one study, it was discovered that magnetic nanoparticles integrated with active drugs on the surface of the structure performed better in terms of drug loading capacity and drug distribution effectiveness than porous hollow magnetic capsules filled with active drugs and then bound with lipids or other polymeric materials.

Scientists from the group studied the anti-cancer effects of graphene-poly(vinylpyrrolidone) nanomaterials (against HeLa, SCC-9, HCT-116, NIH-3T3, and HEK-293 cell lines) and the pH-sensitive drug distribution of the anti-cancer drug doxorubicin (GRP-PVP-DOX) in their study. These composites exhibited dual functionality and were used to study the cytotoxic mechanism for the destruction of cancer cells.

In another investigation, a $\text{Fe}_3\text{O}_4/\text{Cu}_3(\text{BTC})_2$ nanocomposite (BTC = benzene-1,3,5-tricarboxylate) was prepared by fusing Fe_3O_4 nanorods with $\text{Cu}_3(\text{BTC})_2$ nanocrystals (HKUST-1), and nimesulide, an anti-cancer medication that acts as a selective cyclooxygenase-2 (COX-2) inhibitor, was then loaded onto the composite. These nanocomposites have been effectively used for magnetic separation, selective drug delivery, and magnetic resonance imaging. In another study, scientists developed pure mesoporous silica nanoparticles that showed promise as a vehicle for administering targeted medications for MDR cancer treatments.

Researchers developed nanoscale FePt network hollow tablets, which were then lipid-coated and used as magnetic capsules for anti-cancer studies. The aqueous anti-cancer drug has been loaded into the hollow interior cavities of nanosized FePt capsules and delivered to cancer cells without external stimulation. The drug-loaded capsule-coated lipid membrane was successfully directed to the cancer cells using an NdFeB magnet (0.2 T) and killed over 70% of the cancer cells (lung cancer cell line RERF-LC-A1 and gastric cancer cell line MKN-74).

Self-assembly was used to create novel bifunctional magnetic CoFe_2O_4 nanoparticles enclosed with fibrous silica shells. These spherical nanocomposites were used as a potential drug-delivery strategy for chemotherapy against the HeLa cell line due to their mesoporous framework, narrow size distribution, large surface area, good monodispersity, and superparamagnetic characteristics. In green manufacturing of silver nanoparticles, the use of *P. annua* extracts with appropriate concentrations of flavonoids, phenols, and alkaloids as reducing and stabilizing agents for AgNPs was described. The anti-cancer medicine (AgNPs-EDL@Starch) was then delivered using these biogenic AgNPs coated with starch.

Aside from these nanomaterials, others such as Au NPs, Ag NPs, Iron Oxide NPs, Cobalt Ferrites, and Silica NPs have been synthesized and used efficiently as nanomedicine for targeted drug delivery to cancers such as lung cancer, breast cancer, ovarian cancer, and cervical cancer. These findings demonstrated that nanomedicine delivery devices constitute a promising new therapeutic method for cancer therapy. Additional research is needed to transition these "smart" NPs from their experimental phase to therapeutic use.

4. Conclusions

Despite significant advances in the production of nanoparticles for drug delivery, many obstacles remain. Metal NPs are being studied extensively due to their unique properties, which include excellent loading efficiency, size homogeneity, and imaging capabilities. However, the possibility of toxicity severely limits their practical application. As a result, developing materials for carrying drugs with adequate biosafety, excellent biocompatibility, substantial drug loading, and complex circulation is difficult. Natural cell membrane-based materials merit

in-depth investigation for the development of targeted delivery systems, as they are biodegradable, have low immunogenicity, and can be genetically manipulated. Current tactics may be able to overcome obstacles through focused customization and the development of biofilm nanocarriers.

To effectively target a range of cell types, nano-delivery devices can overcome various obstacles. This approach is desirable for enhancing drug transport over barriers and overcoming drug resistance in target cells. However, the challenge still lies in accurately identifying molecular targets and ensuring that these drugs exclusively affect the relevant organs. Furthermore, it is crucial to understand what happens to drugs once they are delivered to the nucleus along with other delicate cellular organelles.

Although nanotargeted treatment has been demonstrated to have therapeutic benefits in cell models and subcutaneous xenograft animal models, its effects in human tissues are rarely investigated. As a result, organoid models could be used in nanotargeted therapeutic research to provide preliminary animal testing data and a more reliable reference for clinical trials. Finally, novel procedures or methodologies, as well as preclinical models, will help expand knowledge of cancer nanomedicines, perhaps speeding their transition from the laboratory to the clinic.

Author Contributions

Conceptualization, B.R.T.; methodology, S.W.; software, B.R.T.; validation, V.A.C.; formal analysis, V.A.C.; data curation, V.A.V.; writing—original draft preparation, B.R.T.; writing—review and editing, D.S.B., V.A.C., AND S.W.; supervision, D.S.B. All authors have read and agreed to the published version of the manuscript.

Institutional Review Board Statement

Not applicable.

Informed Consent Statement

Not applicable.

Data Availability Statement

No new data were created or analyzed in this study. Data sharing is not applicable.

Funding

This research received no external funding.

Acknowledgments

The contributors to this work, whether directly or indirectly, have our sincere gratitude.

Conflicts of Interest

The authors declare no conflict of interest.

References

1. Thuraisingam, S.; Salim, N.; Azmi, I.D.M.; Kassim, N.K.; Basri, H. Development of Nanoemulsion containing *Centella Asiatica* Crude Extract as a Promising Drug Delivery System for Epilepsy Treatment. *Biointerface Res. Appl. Chem.* **2023**, *13*, 17, <https://doi.org/10.33263/BRIAC131.017>.
2. Mohamed, H.H.; Youssef, T.E.; Fadeel, D.A. Magnetic ZnO/CdO Nanocomposite for Effective Drug Delivery System for Cancer Therapy. *Biointerface Res. Appl. Chem.* **2023**, *13*, 60, <https://doi.org/10.33263/BRIAC131.060>.
3. Hossain, K.M.Z.; Patel, U.; Ahmed, I. Development of microspheres for biomedical applications: a review. *Prog. Biomater.* **2015**, *4*, 1-19, <https://doi.org/10.1007/s40204-014-0033-8>.
4. Behera, M. Study of Optical, Thermal, Mechanical and Microstructural Properties of Fullerene/Poly (vinylidene fluoride) Polymer Nanocomposites. *Biointerface Res. Appl. Chem.* **2023**, *13*, 121, <https://doi.org/10.33263/BRIAC132.121>.
5. Vallet-Regi, M.; Rámila, A.; del Real, R.P.; Pérez-Pariente, J. A New Property of MCM-41: Drug Delivery System. *Chem. Mater.* **2001**, *13*, 308-311, <https://doi.org/10.1021/cm0011559>.
6. Vlaskou, D.; Mykhaylyk, O.; Krötz, F.; Hellwig, N.; Renner, R.; Schillinger, U.; Gleich, B.; Heidsieck, A.; Schmitz, G.; Hensel, K.; Plank, C. Magnetic and Acoustically Active Lipospheres for Magnetically Targeted Nucleic Acid Delivery. *Adv. Funct. Mater.* **2010**, *20*, 3881-3894, <https://doi.org/10.1002/adfm.200902388>.
7. Wang, G.; Zhao, D.; Li, N.; Wang, X.; Ma, Y. Drug-loaded poly (ϵ -caprolactone)/Fe₃O₄ composite microspheres for magnetic resonance imaging and controlled drug delivery. *J. Magn. Magn. Mater.* **2018**, *456*, 316-323, <https://doi.org/10.1016/j.jmmm.2018.02.053>.
8. Hashemi, H.; Namazi, H. Understanding the pH dependent fluorescence and doxorubicin release from graphene oxide functionalized citric acid dendrimer as a highly efficient drug delivery system. *Mat. Today Commun.* **2021**, *28*, 102593, <https://doi.org/10.1016/j.mtcomm.2021.102593>.
9. Basavarajappa, P.N.; Hegde, M.M.R.; Rajendrachari, S.; Surendranathan, A.O. Investigation of Structural and Mechanical Properties of Nanostructured TiMgSr Alloy for Biomedical applications. *Biointerface Res. Appl. Chem.* **2023**, *13*, 118, <https://doi.org/10.33263/BRIAC132.118>.
10. Ke, F.; Yuan, Y.-P.; Qiu, L.-G.; Shen, Y.-H.; Xie, A.-J.; Zhu, J.-F.; Tian, X.-Y.; Zhang, L.-D. Facile fabrication of magnetic metal-organic framework nanocomposites for potential targeted drug delivery. *J. Mater. Chem.* **2011**, *21*, 3843-3848, <https://doi.org/10.1039/C0JM01770A>.
11. Lai, P.; Daear, W.; Löbenberg, R.; Prenner, E.J. Overview of the preparation of organic polymeric nanoparticles for drug delivery based on gelatine, chitosan, poly(D,L-lactide-co-glycolic acid) and polyalkylcyanoacrylate. *Colloids Surf. B: Biointerfaces* **2014**, *118*, 154-163, <https://doi.org/10.1016/j.colsurfb.2014.03.017>.
12. Dharmalingam, N.; Vasekaran, M.; Mariappan, R. Design, Cytotoxicity, and Tumor Targeted Drug Delivery of 5Fluorouracil Encapsulated in pH-Sensitive Copolymers GG-g-P (HEMA) Conjugate Riboflavin Thin Film. *Biointerface Res. Appl. Chem.* **2023**, *13*, 285, <https://doi.org/10.33263/BRIAC133.285>.
13. Akentieva, N.; Gizatullin, A.; Sanina, N.; Shkondina, N.; Abramova, K.; Tikhonov, V.; Shram, S.; Aldoshin, S. Intracytoplasmic Trafficking of Nanoparticles based on Hyaluronic Acid and Chitosan for Targeted Delivery of Anti-cancer Drugs. *Biointerface Res. Appl. Chem.* **2023**, *13*, 344, <https://doi.org/10.33263/BRIAC134.344>.
14. Jaiswal, S.; Dutta, P.K.; Kumar, S.; Chawla, R. Chitosan modified by organo-functionalities as an efficient nanoplatform for anti-cancer drug delivery process. *J. Drug Deliv. Sci. Technol.* **2021**, *62*, 102407, <https://doi.org/10.1016/j.jddst.2021.102407>.
15. Tiama, T.M.; Ismail, A.M.; Elhaes, H.; Ibrahim, M.A. Structural and Spectroscopic Studies for Chitosan/Fe₃O₄ Nanocomposites as Glycine Biosensors. *Biointerface Res. Appl. Chem.* **2023**, *13*, 547, <https://doi.org/10.33263/BRIAC136.547>.
16. Schneible, J.D.; Singhal, A.; Lilova, R.L.; Hall, C.K.; Grafmüller, A.; Menegatti, S. Tailoring the Chemical Modification of Chitosan Hydrogels to Fine-Tune the Release of a Synergistic Combination of Chemotherapeutics. *Biomacromolecules* **2019**, *20*, 3126-3141, <https://doi.org/10.1021/acs.biomac.9b00707>.
17. Silva, D.S.; Almeida, A.; Prezotti, F.; Cury, B.; Campana-Filho, S.P.; Sarmiento, B. Synthesis and characterization of 3,6-O,O'- dimyristoyl chitosan micelles for oral delivery of paclitaxel. *Colloids Surf. B: Biointerfaces* **2017**, *152*, 220-228, <https://doi.org/10.1016/j.colsurfb.2017.01.029>.

18. Harutyunyan, L.R.; Lasareva, E.V. Chitosan and its Derivatives: A Step Towards Green Chemistry. *Biointerface Res. Appl. Chem.* **2023**, *13*, 578, <https://doi.org/1.33263/BRIAC136.578>.
19. Du, Y.-Z.; Wang, L.; Yuan, H.; Wei, X.-H.; Hu, F.-Q. Preparation and characteristics of linoleic acid-grafted chitosan oligosaccharide micelles as a carrier for doxorubicin. *Colloids Surf. B: Biointerfaces* **2009**, *69*, 257–263, <https://doi.org/10.1016/j.colsurfb.2008.11.030>.
20. Sharma, D.; Singh, J. Synthesis and Characterization of Fatty Acid Grafted Chitosan Polymer and Their Nanomicelles for Nonviral Gene Delivery Applications. *Bioconjugate Chem.* **2017**, *28*, 2772–2783, <https://doi.org/10.1021/acs.bioconjchem.7b00505>.
21. Layek, B.; Singh, J. Caproic acid grafted chitosan cationic nanocomplexes for enhanced gene delivery: Effect of degree of substitution. *Int. J. Pharm.* **2013**, *447*, 182–191, <https://doi.org/10.1016/j.ijpharm.2013.02.052>.
22. Termsarasab, U.; Cho, H.-J.; Kim, D.H.; Chong, S.; Chung, S.-J.; Shim, C.-K.; Moon, H.T.; Kim, D.-D. Chitosan oligosaccharide–arachidic acid-based nanoparticles for anti-cancer drug delivery. *Int. J. Pharm.* **2013**, *441*, 373–380, <https://doi.org/10.1016/j.ijpharm.2012.11.018>.
23. Motiei, M.; Kashanian, S.; Taherpour, A. Hydrophobic amino acids grafted onto chitosan: a novel amphiphilic chitosan nanocarrier for hydrophobic drugs. *Drug Dev. Ind. Pharm.* **2017**, *43*, 1–11, <https://doi.org/10.1080/03639045.2016.1254240>.
24. Ismail, A.M.; Tiama, T.M.; Farghaly, A.; Elhaes, H.; Ibrahim, M.A. Assessment of the Functionalization of Chitosan/ Iron Oxide Nanoparticles. *Biointerface Res. Appl. Chem.* **2023**, *13*, 582, <https://doi.org/1.33263/BRIAC136.582>.
25. Wang, H.; Yang, Z.; He, Z.; Zhou, C.; Wang, C.; Chen, Y.; Liu, X.; Li, S.; Li, P. Self-assembled amphiphilic chitosan nanomicelles to enhance the solubility of quercetin for efficient delivery. *Colloids Surf. B: Biointerfaces* **2019**, *179*, 519–526, <https://doi.org/10.1016/j.colsurfb.2019.04.007>.
26. Almeida, A.; Silva, D.; Gonçalves, V.; Sarmiento, B. Synthesis and characterization of chitosan-grafted-polycaprolactone micelles for modulate intestinal paclitaxel delivery. *Drug Deliv. Transl. Res.* **2018**, *8*, 387–397, <https://doi.org/10.1007/s13346-017-0357-8>.
27. Gu, C.; Le, V.; Lang, M.; Liu, J. Preparation of polysaccharide derivatives chitosan-graft-poly(ϵ -caprolactone) amphiphilic copolymer micelles for 5-fluorouracil drug delivery. *Colloids Surf. B: Biointerfaces* **2014**, *116*, 745–750, <https://doi.org/10.1016/j.colsurfb.2014.01.026>.
28. Muddineti, O.S.; Shah, A.; Rompicharla, S.V.K.; Ghosh, B.; Biswas, S. Cholesterol-grafted chitosan micelles as a nanocarrier system for drug-siRNA co-delivery to the lung cancer cells. *Int. J. Biol. Macromol.* **2018**, *118*, 857–863, <https://doi.org/10.1016/j.ijbiomac.2018.06.114>.
29. Mu, Y.; Fu, Y.; Li, J.; Yu, X.; Li, Y.; Wang, Y.; Wu, X.; Zhang, K.; Kong, M.; Feng, C.; Chen, X. Multi-functional quercetin conjugated chitosan nano-micelles with P-gp inhibition and permeation enhancement of anti-cancer drug. *Carbohydr. Polym.* **2019**, *203*, 10–18, <https://doi.org/10.1016/j.carbpol.2018.09.020>.
30. de Oliveira Pedro, R.; Hoffmann, S.; Pereira, S.; Goycoolea, F.M.; Schmitt, C.C.; Neumann, M.G. Self-assembled amphiphilic chitosan nanoparticles for quercetin delivery to breast cancer cells. *Eur. J. Pharm. Biopharm.* **2018**, *131*, 203–210, <https://doi.org/10.1016/j.ejpb.2018.08.009>.
31. de Oliveira Pedro, R.; Goycoolea, F.M.; Pereira, S.; Schmitt, C.C.; Neumann, M.G. Synergistic effect of quercetin and pH-responsive DEAE-chitosan carriers as drug delivery system for breast cancer treatment. *Int. J. Biol. Macromol.* **2018**, *106*, 579–586, <https://doi.org/10.1016/j.ijbiomac.2017.08.056>.
32. Almeida, A.; Araújo, M.; Novoa-Carballal, R.; Andrade, F.; Gonçalves, H.; Reis, R.L.; Lúcio, M.; Schwartz, S.; Sarmiento, B. Novel amphiphilic chitosan micelles as carriers for hydrophobic anti-cancer drugs. *Mat. Sci. Eng.: C* **2020**, *112*, 110920, <https://doi.org/10.1016/j.msec.2020.110920>.
33. Silva, D.S.; M. dos Santos, D.; Almeida, A.; Marchiori, L.; Campana-Filho, S.P.; Ribeiro, S.J.L.; Sarmiento, B. *N*-(2-Hydroxy)-propyl-3-trimethylammonium, *O*-Mysristoyl Chitosan Enhances the Solubility and Intestinal Permeability of Anti-cancer Curcumin. *Pharmaceutics* **2018**, *10*, 245, <https://doi.org/10.3390/pharmaceutics10040245>.
34. Kumar Mehata, A.; Bharti, S.; Singh, P.; Viswanadh, M.K.; Kumari, L.; Agrawal, P.; Singh, S.; Koch, B.; Muthu, M.S. Trastuzumab decorated TPGS-g-chitosan nanoparticles for targeted breast cancer therapy. *Colloids Surf. B: Biointerfaces* **2019**, *173*, 366–377, <https://doi.org/10.1016/j.colsurfb.2018.10.007>.
35. Naruphontjirakul, P.; Viravaidya-Pasuwat, K. Development of anti-HER2-targeted doxorubicin–core-shell chitosan nanoparticles for the treatment of human breast cancer. *Int. J. Nanomed.* **2019**, *14*, 4105–4121, <https://doi.org/10.2147/IJN.S198552>.

36. Sabra, R.; Billa, N.; Roberts, C.J. Cetuximab-conjugated chitosan-pectinate (modified) composite nanoparticles for targeting colon cancer. *Int. J. Pharm.* **2019**, *572*, 118775, <https://doi.org/10.1016/j.ijpharm.2019.118775>.
37. Qu, C.; Li, J.; Zhou, Y.; Yang, S.; Chen, W.; Li, F.; You, B.; Liu, Y.; Zhang, X. Targeted Delivery of Doxorubicin via CD147-Mediated ROS/pH Dual-Sensitive Nanomicelles for the Efficient Therapy of Hepatocellular Carcinoma. *AAPS J.* **2018**, *20*, 34, <https://doi.org/10.1208/s12248-018-0195-8>.
38. Shoaib, M.; Bahadur, A.; Saeed, A.; ur Rahman, M.S.; Naseer, M.M. Biocompatible, pH-responsive, and biodegradable polyurethanes as smart anti-cancer drug delivery carriers. *React. Funct. Polym.* **2018**, *127*, 153–160, <https://doi.org/10.1016/j.reactfunctpolym.2018.04.010>.
39. Fahr, A.; Liu, X. Drug delivery strategies for poorly water-soluble drugs. *Expert Opin. Drug Deliv.* **2007**, *4*, 403-416, <https://doi.org/10.1517/17425247.4.4.403>.
40. Prasad, M.S.N.A.; Puthalapattu, R.P.; Babu, B.K.; Kanchi, S. Synthesis and Spectral Characterization of Novel Schiff Base and Fe(II) Complex: Evaluation of Antibacterial, Antifungal, and Anti-cancer Properties. *Lett. Appl. NanoBioScience* **2023**, *12*, 41, <https://doi.org/10.33263/LIANBS122.041>.
41. He, Q.; Gao, Y.; Zhang, L.; Zhang, Z.; Gao, F.; Ji, X.; Li, Y.; Shi, J. A pH-responsive mesoporous silica nanoparticles-based multidrug delivery system for overcoming multidrug resistance. *Biomaterials* **2011**, *32*, 7711-7720, <https://doi.org/10.1016/j.biomaterials.2011.06.066>.
42. Wang, L.-S.; Wu, L.-C.; Lu, S.-Y.; Chang, L.-L.; Teng, I.T.; Yang, C.-M.; Ho, J.-a.A. Biofunctionalized Phospholipid-Capped Mesoporous Silica Nanoshuttles for Targeted Drug Delivery: Improved Water Suspensibility and Decreased Nonspecific Protein Binding. *ACS Nano* **2010**, *4*, 4371-4379, <https://doi.org/10.1021/nn901376h>.
43. Li, C.; Hou, Z.; Dai, Y.; Yang, D.; Cheng, Z.; Ma, P.a.; Lin, J. A facile fabrication of upconversion luminescent and mesoporous core-shell structured β -NaYF₄:Yb³⁺, Er³⁺@mSiO₂ nanocomposite spheres for anti-cancer drug delivery and cell imaging. *Biomater. Sci.* **2013**, *1*, 213-223, <https://doi.org/10.1039/C2BM00087C>.
44. Zhang, F.; Shi, Y.; Sun, X.; Zhao, D.; Stucky, G.D. Formation of Hollow Upconversion Rare-Earth Fluoride Nanospheres: Nanoscale Kirkendall Effect During Ion Exchange. *Chem. Mater.* **2009**, *21*, 5237-5243, <https://doi.org/10.1021/cm902231s>.
45. Yang, D.; Kang, X.; Ma, P.a.; Dai, Y.; Hou, Z.; Cheng, Z.; Li, C.; Lin, J. Hollow structured upconversion luminescent NaYF₄:Yb³⁺, Er³⁺ nanospheres for cell imaging and targeted anti-cancer drug delivery. *Biomaterials* **2013**, *34*, 1601-1612, <https://doi.org/10.1016/j.biomaterials.2012.11.004>.
46. Fuchigami, T.; Kawamura, R.; Kitamoto, Y.; Nakagawa, M.; Namiki, Y. A magnetically guided anti-cancer drug delivery system using porous FePt capsules. *Biomaterials* **2012**, *33*, 1682-1687, <https://doi.org/10.1016/j.biomaterials.2011.11.016>.
47. Khanmohammadi, A.; Rashidi, V.; Sadighian, S. Reduced Graphene Oxide/Silica Nanocomposite as Anti-cancer Drug Delivery Nanocarrier. *Biointerface Res. Appl. Chem.* **2023**, *13*, 383, <https://doi.org/10.33263/BRIAC134.383>.
48. Nimshi, R.E.; Vijaya, J.J.; Kennedy, L.J.; Selvamani, P.S.; Bououdina, M.; Sophia, P.J. Effective microwave assisted synthesis of CoFe₂O₄@TiO₂@rGO ternary nanocomposites for the synergic sonophotocatalytic degradation of tetracycline and c antibiotics. *Ceram. Int.* **2023**, *49*, 13762-13773, <https://doi.org/10.1016/j.ceramint.2022.12.254>.
49. Song, J.; Zhang, J.; Zada, A.; Ma, Y.; Qi, Z. CoFe₂O₄/NiFe₂O₄ S-scheme composite for photocatalytic decomposition of antibiotic contaminants. *Ceram. Int.* **2023**, *49*, 12327-12333, <https://doi.org/10.1016/j.ceramint.2022.12.088>.
50. Wu, L.; Xiao, Q.; Li, Z.; Lei, G.; Zhang, P.; Wang, L. CoFe₂O₄/C composite fibers as anode materials for lithium-ion batteries with stable and high electrochemical performance. *Solid State Ion.* **2012**, *215*, 24–28, <https://doi.org/10.1016/j.ssi.2012.03.044>.
51. He, Y.; Wang, Y.; Yang, X.; Xie, S.; Yuan, R.; Chai, Y. Metal Organic Frameworks Combining CoFe₂O₄ Magnetic Nanoparticles as Highly Efficient SERS Sensing Platform for Ultrasensitive Detection of N-Terminal Pro-Brain Natriuretic Peptide. *ACS Appl. Mater. Interfaces* **2016**, *8*, 7683–7690, <https://doi.org/10.1021/acsami.6b01112>.
52. Cai, B.; Zhao, M.; Ma, Y.; Ye, Z.; Huang, J. Bioinspired Formation of 3D Hierarchical CoFe₂O₄ Porous Microspheres for Magnetic-Controlled Drug Release. *ACS Appl. Mater. Interfaces* **2015**, *7*, 1327–1333, <https://doi.org/10.1021/am507689a>.

53. Fan, H.; Li, B.; Shi, Z.; Zhao, L.; Wang, K.; Qiu, D. A fibrous morphology silica- CoFe₂O₄ nanocarrier for anti-cancer drug delivery. *Ceram. Int.* **2018**, *44*, 2345–2350, <https://doi.org/10.1016/j.ceramint.2017.10.201>.
54. Shanwaz, M.M.; Shyam, P. Synthesis of Silver Nanoparticles from *Vitex negundo* Plant by Green Method and their Bactericidal Effects. *Lett. Appl. NanoBioScience* **2023**, *12*, 59, <https://doi.org/10.33263/LIANBS122.059>.
55. Gul, A.R.; Shaheen, F.; Rafique, R.; Bal, J.; Waseem, S.; Park, T.J. Grass-mediated biogenic synthesis of silver nanoparticles and their drug delivery evaluation: A biocompatible anti-cancer therapy. *Chem. Eng. J.* **2020**, *407*, 127202, <https://doi.org/10.1016/j.cej.2020.127202>.
56. Ozel, F.; Kockar, H.; Karaagac, O. Growth of Iron Oxide Nanoparticles by Hydrothermal Process: Effect of Reaction Parameters on the Nanoparticle Size. *J. Supercond. Nov. Magn.* **2015**, *28*, 823–829, <https://doi.org/10.1007/s10948-014-2707-9>.
57. Suk, J.S.; Xu, Q.; Kim, N.; Hanes, J.; Ensign, L.M. PEGylation as a strategy for improving nanoparticle-based drug and gene delivery. *Adv. Drug Deliv. Rev.* **2016**, *99*, 28–51, <https://doi.org/10.1016/j.addr.2015.09.012>.
58. Yu, P.; Xia, X.-M.; Wu, M.; Cui, C.; Zhang, Y.; Liu, L.; Wu, B.; Wang, C.-X.; Zhang, L.-J.; Zhou, X.; Zhuo, R.-X.; Huang, S.-W. Folic acid-conjugated iron oxide porous nanorods loaded with doxorubicin for targeted drug delivery. *Colloids Surf. B: Biointerfaces* **2014**, *120*, 142–151, <https://doi.org/10.1016/j.colsurfb.2014.05.018>.
59. Ay, A.N.; Konuk, D.; Zümreoğlu-Karan, B. Magnetic nanocomposites with drug-intercalated layered double hydroxide shell supported on commercial magnetite and laboratory-made magnesium ferrite core materials. *Mater. Sci. Eng.: C* **2011**, *31*, 851–857, <https://doi.org/10.1016/j.msec.2011.01.007>.
60. Pan, D.; Zhang, H.; Zhang, T.; Duan, X. A novel organic–inorganic microhybrids containing anti-cancer agent doxifluridine and layered double hydroxides: Structure and controlled release properties. *Chem. Eng. Sci.* **2010**, *65*, 3762–3771, <https://doi.org/10.1016/j.ces.2010.03.013>.
61. Ferrari, I.V.; Narducci, R.; Prestopino, G.; Costantino, F.; Mattocchia, A.; Di Giamberardino, L.; Nocchetti, M.; Di Vona, M.L.; Paolone, A.; Bini, M.; Pezzilli, R.; Borromeo, I.; Beninati, S.; Medaglia, P.G. Layered Double Hydroxides as a Drug Delivery Vehicle for S-Allyl-Mercapto-Cysteine (SAMC). *Processes* **2021**, *9*, 1819, <https://doi.org/10.3390/pr9101819>.
62. Ay, A.N.; Konuk, D.; Zümreoğlu-Karan, B. Magnetic nanocomposites with drug-intercalated layered double hydroxide shell supported on commercial magnetite and laboratory-made magnesium ferrite core materials. *Mater. Sci. Eng.: C* **2011**, *31*, 851–857, <http://dx.doi.org/10.1016/j.msec.2011.01.007>.
63. Bindhya, K.P.; Uma Maheswari, P.; Meera Sheriffa Begum, K.M. Milk protein inspired multi-functional magnetic carrier targeting progesterone receptors: Improved anti-cancer potential of soybean-derived genistein against breast and ovarian cancers. *Mater. Chem. Phys.* **2021**, *272*, 125055, <https://doi.org/10.1016/j.matchemphys.2021.125055>.
64. Yang, L.; Tian, J.; Meng, J.; Zhao, R.; Li, C.; Ma, J.; Jin, T. Modification and Characterization of Fe₃O₄ Nanoparticles for Use in Adsorption of Alkaloids. *Molecules* **2018**, *23*, 562, <https://doi.org/10.3390/molecules23030562>.
65. Abdussalam-Mohammed, W.; Abraheem, M.S.; Mezoughi, A.B.; Mohamed, L.; Alwahsh, M.A.A. Comparative Analysis of Novel Iron Oxide Nanoparticles Synthesized by Different Approaches with Evaluation of Their Antibacterial Activities. *Biointerface Res. Appl. Chem.* **2023**, *13*, 317, <https://doi.org/10.33263/BRIAC134.317>.
66. Wang, L.; Zhang, H.; Qin, A.; Jin, Q.; Tang, B.Z.; Ji, J. Theranostic hyaluronic acid prodrug micelles with aggregation-induced emission characteristics for targeted drug delivery. *Sci. China Chem.* **2016**, *59*, 1609–1615, <https://doi.org/10.1007/s11426-016-0246-9>.
67. Xu, Z.; Li, C.; Kang, X.; Yang, D.; Yang, P.; Hou, Z.; Lin, J. Synthesis of a Multi-functional Nanocomposite with Magnetic, Mesoporous, and Near-IR Absorption Properties. *J. Phys. Chem. C* **2010**, *114*, 16343–16350, <https://doi.org/10.1021/jp106325c>.
68. Zhu, Y.; Kockrick, E.; Ikoma, T.; Hanagata, N.; Kaskel, S. An Efficient Route to Rattle-Type Fe₃O₄@SiO₂ Hollow Mesoporous Spheres Using Colloidal Carbon Spheres Templates. *Chem. Mater.* **2009**, *21*, 2547–2553, <https://doi.org/10.1021/cm900956j>.
69. Bae, Y.H.; Park, K. Targeted drug delivery to tumors: Myths, reality and possibility. *J. Control. Release* **2011**, *153*, 198–205, <https://doi.org/10.1016/j.jconrel.2011.06.001>.

70. Uribe Madrid, S.I.; Pal, U.; Kang, Y.S.; Kim, J.; Kwon, H.; Kim, J. Fabrication of Fe₃O₄@mSiO₂ Core-Shell Composite Nanoparticles for Drug Delivery Applications. *Nanoscale Res. Lett.* **2015**, *10*, 217, <https://doi.org/10.1186/s11671-015-0920-5>.
71. Xiao, X.; Yang, H.; Jiang, P.; Chen, Z.; Ji, C.; Nie, L. Multi-Functional Fe₃O₄@mSiO₂-AuNCs Composite Nanoparticles Used as Drug Delivery System. *J. Biomed. Nanotechnol.* **2017**, *13*, 1292–1299, <https://doi.org/10.1166/jbn.2017.2417>.
72. Tian, B.-S.; Yang, C. Thermo-Sensitive Poly(*N*-Isopropylacrylamide)/Mesoporous Silica Nanocomposites as Controlled Delivery Carriers: Loading and Release Behaviors for Drug Ibuprofen. *J. Nanosci. Nanotechnol.* **2011**, *11*, 1871-1879, <https://doi.org/10.1166/JNN.2011.3543>.
73. Lue, S.J.; Chen, B.-W.; Shih, C.-M.; Chou, F.-Y.; Lai, J.-Y.; Chiu, W.-Y. Micron- and Nano-sized Poly(*N*-isopropylacrylamide-co-acrylic acid) Latex Syntheses and Their Applications for Controlled Drug Release. *J. Nanosci. Nanotechnol.* **2013**, *13*, 5305-5315, <https://doi.org/10.1166/jnn.2013.7532>.
74. Hofmann, C.H.; Schönhoff, M. Dynamics and distribution of aromatic model drugs in the phase transition of thermoreversible poly(*N*-isopropylacrylamide) in solution. *Colloid Polym. Sci.* **2012**, *290*, 689–698, <https://doi.org/10.1007/s00396-011-2577-7>.
75. Wang, W.; Tian, X.; Feng, Y.; Cao, B.; Yang, W.; Zhang, L. Thermally On–Off Switching Membranes Prepared by Pore-Filling Poly(*N*-isopropylacrylamide) Hydrogels. *Ind. Eng. Chem. Res.* **2010**, *49*, 1684-1690, <https://doi.org/10.1021/ie9008666>.
76. Zeinali, E.; Haddadi-Asl, V.; Roghani-Mamaqani, H. Synthesis of dual thermo- and pH-sensitive poly(*N*-isopropylacrylamide-co-acrylic acid)-grafted cellulose nanocrystals by reversible addition-fragmentation chain transfer polymerization. *J. Biomed. Mater. Res. A* **2018**, *106*, 231-243, <https://doi.org/10.1002/jbm.a.36230>.
77. Tuncelli, G.; Ay, A.N.; Zümreoglu-Karan, B. 5-Fluorouracil intercalated iron oxide@layered double hydroxide core-shell nanocomposites with isotropic and anisotropic architectures for shape-selective drug delivery applications. *Mater. Sci. Eng.: C* **2015**, *55*, 562–568, <https://doi.org/10.1016/j.msec.2015.06.001>.
78. Ruiz-Hernández, E.; López-Noriega, A.; Arcos, D.; Vallet-Regí, M. Mesoporous magnetic microspheres for drug targeting. *Solid State Sci.* **2008**, *10*, 421-426, <https://doi.org/10.1016/j.solidstatesciences.2007.11.026>.
79. Torabi, M.; Aghanejad, A.; Savadi, P.; Barzegari, A.; Omid, Y.; Barar, J. Fabrication of mesoporous silica nanoparticles for targeted delivery of sunitinib to ovarian cancer cells. *Bioimpacts* **2023**, *13*, 255-267, <https://doi.org/10.34172/bi.2023.25298>.
80. Radu, D.R.; Lai, C.Y.; Jeftinija, K.; Rowe, E.W.; Jeftinija, S.; Lin, V.S.-Y. A Polyamidoamine Dendrimer-Capped Mesoporous Silica Nanosphere-Based Gene Transfection Reagent. *J. Am. Chem. Soc.* **2004**, *126*, 13216-13217, <https://doi.org/10.1021/ja046275m>.
81. Arruebo, M.; Fernández-Pacheco, R.; Irusta, S.; Arbiol, J.; Ibarra, M.R.; Santamaría, J. Sustained release of doxorubicin from zeolite-magnetite nanocomposites prepared by mechanical activation. *Nanotechnology* **2006**, *17*, 4057, <https://doi.org/10.1088/0957-4484/17/16/011>.
82. Lai, C.-Y.; Trewyn, B.G.; Jeftinija, D.M.; Jeftinija, K.; Xu, S.; Jeftinija, S.; Lin, V.S.Y. A Mesoporous Silica Nanosphere-Based Carrier System with Chemically Removable CdS Nanoparticle Caps for Stimuli-Responsive Controlled Release of Neurotransmitters and Drug Molecules. *J. Am. Chem. Soc.* **2003**, *125*, 4451-4459, <https://doi.org/10.1021/ja028650l>.
83. Lu, J.; Liang, M.; Zink, J.I.; Tamanoi, F. Mesoporous Silica Nanoparticles as a Delivery System for Hydrophobic Anti-cancer Drugs. *Small* **2007**, *3*, 1341–1346, <https://doi.org/10.1002/smll.200700005>.
84. Wang, G.; Chen, G.; Wei, Z.; Dong, X.; Qi, M. Multi-functional Fe₃O₄/graphene oxide nanocomposites for magnetic resonance imaging and drug delivery. *Mater. Chem. Phys.* **2013**, *141*, 997-1004, <https://doi.org/10.1016/j.matchemphys.2013.06.054>.
85. Jafarizad, A.; Aghanejad, A.; Sevim, M.; Metin, Ö.; Barar, J.; Omid, Y.; Ekin, D. Gold Nanoparticles and Reduced Graphene Oxide-Gold Nanoparticle Composite Materials as Covalent Drug Delivery Systems for Breast Cancer Treatment. *ChemistrySelect* **2017**, *2*, 6663–6672, <https://doi.org/10.1002/slct.201701178>.
86. Sagir, T.; Huysal, M.; Senel, M.; Isik, S.; Burgucu, N.; Tabakoglu, O.; Zaim, M. Folic acid conjugated PAMAM-modified mesoporous silica-coated superparamagnetic iron oxide nanoparticles for potential cancer therapy. *J. Colloid Interface Sci.* **2022**, *625*, 711-721, <https://doi.org/10.1016/j.jcis.2022.06.069>.

87. Sharma, A.; Sharma, S.; Khuller, G.K. Lectin-functionalized poly (lactide-co-glycolide) nanoparticles as oral/aerosolized antitubercular drug carriers for treatment of tuberculosis. *J. Antimicrob. Chemother.* **2004**, *54*, 761–766, <https://doi.org/10.1093/jac/dkh411>.
88. Shargh, V.H.; Hondermarck, H.; Liang, M. Antibody-targeted biodegradable nanoparticles for cancer therapy. *Nanomedicine* **2016**, *11*, 63-79, <https://doi.org/10.2217/nnm.15.186>.
89. Yuan, X.; Wu, H.; Xu, H.; Han, N.; Chu, Q.; Yu, S.; Chen, Y.; Wu, K. Meta-analysis reveals the correlation of Notch signaling with non-small cell lung cancer progression and prognosis. *Sci. Rep.* **2015**, *5*, 10338, <https://doi.org/10.1038/srep10338>.
90. Kang, B.K.; Chon, S.K.; Kim, S.H.; Jeong, S.Y.; Kim, M.S.; Cho, S.H.; Lee, H.B.; Khang, G. Controlled release of paclitaxel from microemulsion containing PLGA and evaluation of anti-tumor activity in vitro and in vivo. *Int. J. Pharm.* **2004**, *286*, 147-156, <https://doi.org/10.1016/j.ijpharm.2004.08.008>.
91. Patel, J.; Amrutiya, J.; Bhatt, P.; Javia, A.; Jain, M.; Misra, A. Targeted delivery of monoclonal antibody conjugated docetaxel loaded PLGA nanoparticles into EGFR overexpressed lung tumour cells. *J. Microencapsul.* **2018**, *35*, 204-217, <https://doi.org/10.1080/02652048.2018.1453560>.
92. Rivera-Hernández, G.; Antunes-Ricardo, M.; Martínez-Morales, P.; Sánchez, M.L. Polyvinyl alcohol based-drug delivery systems for cancer treatment. *Int. J. Pharm.* **2021**, *600*, 120478, <https://doi.org/10.1016/j.ijpharm.2021.120478>.
93. Qi, S.-S.; Sun, J.-H.; Yu, H.-H.; Yu, S.-Q. Co-delivery nanoparticles of anti-cancer drugs for improving chemotherapy efficacy. *Drug Deliv.* **2017**, *24*, 1909-1926, <https://doi.org/10.1080/10717544.2017.1410256>.
94. Hu, C.-M.J.; Aryal, S.; Zhang, L. Nanoparticle-assisted combination therapies for effective cancer treatment. *Ther. Deliv.* **2010**, *1*, 323–334, <https://doi.org/10.4155/tde.10.13>.
95. Wang, C.; Hu, Q.; Shen, H.-M. Pharmacological inhibitors of autophagy as novel cancer therapeutic agents. *Pharm. Res.* **2016**, *105*, 164–175, <https://doi.org/10.1016/j.phrs.2016.01.028>.
96. Wang, H.; Zhao, Y.; Wu, Y.; Hu, Y.-L.; Nan, K.; Nie, G.; Chen, H. Enhanced anti-tumor efficacy by co-delivery of doxorubicin and paclitaxel with amphiphilic methoxy PEG-PLGA copolymer nanoparticles. *Biomaterials* **2011**, *32*, 8281–8290, <https://doi.org/10.1016/j.biomaterials.2011.07.032>.
97. Yan, T.; Li, D.; Li, J.; Cheng, F.; Cheng, J.; Huang, Y.; He, J. Effective co-delivery of doxorubicin and curcumin using a glycyrrhetic acid-modified chitosan-cystamine-poly(ϵ -caprolactone) copolymer micelle for combination cancer chemotherapy. *Colloids Surf. B: Biointerfaces* **2016**, *145*, 526–538, <https://doi.org/10.1016/j.colsurfb.2016.05.070>.
98. Zhang, R.X.; Cai, P.; Zhang, T.; Chen, K.; Li, J.; Cheng, J.; Pang, K.S.; Adissu, H.A.; Rauth, A.M.; Wu, X.Y. Polymer–lipid hybrid nanoparticles synchronize pharmacokinetics of co-encapsulated doxorubicin–mitomycin C and enable their spatiotemporal co-delivery and local bioavailability in breast tumor. *Nanomed.: Nanotechnol. Biol. Med.* **2016**, *12*, 1279–1290, <https://doi.org/10.1016/j.nano.2015.12.383>.
99. Ma, D.; Zhou, X.-Y.; Yang, Y.-F.; You, Y.; Liu, Z.-H.; Lin, J.-T.; Liu, T.; Xue, W. UV Cross-Linked Redox-Responsive Hydrogels for Co-Delivery of Hydrophilic and Hydrophobic Drugs. *Sci. Adv. Mater.* **2013**, *5*, 1307–1315, <https://doi.org/10.1166/sam.2013.1587>.
100. Lee, A.L.Z.; Wang, Y.; Cheng, H.Y.; Pervaiz, S.; Yang, Y.Y. The co-delivery of paclitaxel and Herceptin using cationic micellar nanoparticles. *Biomaterials* **2009**, *30*, 919–927, <https://doi.org/10.1016/j.biomaterials.2008.10.062>.
101. Zhang, F.; Li, M.; Su, Y.; Zhou, J.; Wang, W. A dual-targeting drug co-delivery system for tumor chemo- and gene combined therapy. *Mater. Sci. Eng.: C* **2016**, *64*, 208–218, <https://doi.org/10.1016/j.msec.2016.03.083>.
102. Xu, Q.; Leong, J.; Chua, Q.Y.; Chi, Y.T.; Chow, P.K.-H.; Pack, D.W.; Wang, C.-H. Combined modality doxorubicin-based chemotherapy and chitosan-mediated p53 gene therapy using double-walled microspheres for treatment of human hepatocellular carcinoma. *Biomaterials* **2013**, *34*, 5149–5162, <https://doi.org/10.1016/j.biomaterials.2013.03.044>.
103. Guo, Y.; He, W.; Yang, S.; Zhao, D.; Li, Z.; Luan, Y. Co-delivery of docetaxel and verapamil by reduction-sensitive PEG-PLGA-SS-DTX conjugate micelles to reverse the multidrug resistance of breast cancer. *Colloids Surf. B: Biointerfaces* **2017**, *151*, 119–127, <https://doi.org/10.1016/j.colsurfb.2016.12.012>.
104. Jia, H.-Z.; Zhang, W.; Zhu, J.-Y.; Yang, B.; Chen, S.; Chen, G.; Zhao, Y.-F.; Feng, J.; Zhang, X.-Z. Hyperbranched–hyperbranched polymeric nanoassembly to mediate controllable co-delivery of siRNA

- and drug for synergistic tumor therapy. *J. Control. Release* **2015**, *216*, 9–17, <https://doi.org/10.1016/j.jconrel.2015.08.006>.
105. Sriraman, S.K.; Zhang, Y.; Luther, E.; Lengyel, E.; Torchilin, V.; Torchilin, V. Abstract 4416: Reversal of chemoresistance in ovarian cancer cells by the liposomal co-delivery of MDR inhibitors and paclitaxel. *Cancer Res.* **2015**, *75*, 4416, <https://doi.org/10.1158/1538-7445.AM2015-4416>.
106. Xu, J.; Zhu, X.; Qiu, L. Polyphosphazene vesicles for co-delivery of doxorubicin and chloroquine with enhanced anti-cancer efficacy by drug resistance reversal. *Int. J. Pharm.* **2016**, *498*, 70–81, <https://doi.org/10.1016/j.ijpharm.2015.12.003>.
107. Suo, A.; Qian, J.; Zhang, Y.; Liu, R.; Xu, W.; Wang, H. Comb-like amphiphilic polypeptide-based copolymer nanomicelles for co-delivery of doxorubicin and P-gp siRNA into MCF-7 cells. *Mater. Sci. Eng.: C* **2016**, *62*, 564–573, <https://doi.org/10.1016/j.msec.2016.02.007>.
108. He, C.; Lu, K.; Liu, D.; Lin, W. Nanoscale Metal–Organic Frameworks for the Co-Delivery of Cisplatin and Pooled siRNAs to Enhance Therapeutic Efficacy in Drug-Resistant Ovarian Cancer Cells. *J. Am. Chem. Soc.* **2014**, *136*, 5181–5184, <https://doi.org/10.1021/ja4098862>.
109. Peng, Z.; Chang, Q.; Xing, M.; Lu, F. Active Hydrophilic Graphene Oxide Nanocomposites Delivery Mediated by Adipose-Derived Stem Cell for Elevated Photothermal Therapy of Breast Cancer. *Int. J. Nanomed.* **2023**, *18*, 971–986, <https://doi.org/10.2147/IJN.S380029>.
110. Hao, Y.; Zhang, B.; Zheng, C.; Ji, R.; Ren, X.; Guo, F.; Sun, S.; Shi, J.; Zhang, H.; Zhang, Z.; Wang, L.; Zhang, Y. The tumor-targeting core–shell structured DTX-loaded PLGA@Au nanoparticles for chemo-photothermal therapy and X-ray imaging. *J. Control. Release* **2015**, *220*, 545–555, <https://doi.org/10.1016/j.jconrel.2015.11.016>.
111. Yao, X.; Chen, L.; Chen, X.; Xie, Z.; Ding, J.; He, C.; Zhang, J.; Chen, X. pH-responsive metallo-supramolecular nanogel for synergistic chemo-photodynamic therapy. *Acta Biomater.* **2015**, *25*, 162–171, <https://doi.org/10.1016/j.actbio.2015.07.024>.
112. Chen, W.-H.; Luo, G.-F.; Qiu, W.-X.; Lei, Q.; Liu, L.-H.; Wang, S.-B.; Zhang, X.-Z. Mesoporous silica-based versatile theranostic nanoplatform constructed by layer-by-layer assembly for excellent photodynamic/chemo therapy. *Biomaterials* **2017**, *117*, 54–65, <https://doi.org/10.1016/j.biomaterials.2016.11.057>.
113. Patel, N.R.; Rathi, A.; Mongayt, D.; Torchilin, V.P. Reversal of multidrug resistance by co-delivery of tariquidar (XR9576) and paclitaxel using long-circulating liposomes. *Int. J. Pharm.* **2011**, *416*, 296–299, <https://doi.org/10.1016/j.ijpharm.2011.05.082>.
114. Wu, J.; Lu, Y.; Lee, A.; Pan, X.; Yang, X.; Zhao, X.; Lee, R.J. Reversal of multidrug resistance by transferrin-conjugated liposomes co-encapsulating doxorubicin and verapamil. *J. Pharm. Pharm. Sci.* **2007**, *10*, 350–357.
115. He, C.; Tang, Z.; Tian, H.; Chen, X. Co-delivery of chemotherapeutics and proteins for synergistic therapy. *Adv. Drug Deliv. Rev.* **2016**, *98*, 64–76, <https://doi.org/10.1016/j.addr.2015.10.021>.
116. Li, J.-M.; Wang, Y.-Y.; Zhao, M.-X.; Tan, C.-P.; Li, Y.-Q.; Le, X.-Y.; Ji, L.-N.; Mao, Z.-W. Multi-functional QD-based co-delivery of siRNA and doxorubicin to HeLa cells for reversal of multidrug resistance and real-time tracking. *Biomaterials* **2012**, *33*, 2780–2790, <https://doi.org/10.1016/j.biomaterials.2011.12.035>.
117. Chen, D.; Liu, X.; Lu, X.; Tian, J. Nanoparticle drug delivery systems for synergistic delivery of tumor therapy. *Front. Pharmacol.* **2023**, *14*, 1111991, <https://doi.org/10.3389/fphar.2023.1111991>.
118. Duan, X.; Xiao, J.; Yin, Q.; Zhang, Z.; Yu, H.; Mao, S.; Li, Y. Smart pH-Sensitive and Temporal-Controlled Polymeric Micelles for Effective Combination Therapy of Doxorubicin and Disulfiram. *ACS Nano* **2013**, *7*, 5858–5869, <https://doi.org/10.1021/nn4010796>.

Publisher’s Note & Disclaimer

The statements, opinions, and data presented in this publication are solely those of the individual author(s) and contributor(s) and do not necessarily reflect the views of the publisher and/or the editor(s). The publisher and/or the editor(s) disclaim any responsibility for the accuracy, completeness, or reliability of the content. Neither the publisher nor the editor(s) assume any legal liability for any errors, omissions, or consequences arising from the use of the information presented in this publication. Furthermore, the publisher and/or the editor(s) disclaim any liability for any injury, damage, or loss to persons or property that may result from the use of any ideas, methods, instructions, or products mentioned in the content. Readers are encouraged to independently verify any

information before relying on it, and the publisher assumes no responsibility for any consequences arising from the use of materials contained in this publication.